



FULL ARTICLE

Journal of
Food Biochemistry

WILEY

Pithecellobium dulce fruit extract mitigates cyclophosphamide-mediated toxicity by regulating proinflammatory cytokines

Suresh Sulekha Dhanisha | Sudarsanan Drishya | Chandrasekharan Guruvayoorappan

Laboratory of Immunopharmacology and Experimental Therapeutics, Division of Cancer Research Regional Cancer Centre (Research Centre, University of Kerala), Thiruvananthapuram, India

Correspondence

Chandrasekharan Guruvayoorappan, Laboratory of Immunopharmacology and Experimental Therapeutics, Division of Cancer Research (Regional Cancer Centre, University of Kerala), Thiruvananthapuram 695 011, Kerala, India.
Email: immunopharmacologyrcc@gmail.com; gururcctvm@gmail.com

Abstract

Pithecellobium dulce (Family: Fabaceae) is an edible fruit widely used in Asian-Pacific region. In the present study, we had investigated the protective effect of *P. dulce* fruit extract in mitigating harmful effects of the chemotherapeutic drug, cyclophosphamide (CTX). Our results showed that *P. dulce* treatment could significantly ($p < .01$) overcome CTX-induced immunosuppression accompanied with urotoxicity, hepatotoxicity, and nephrotoxicity in experimental animals. This was supported by histopathological data which proved that toxic effects of CTX in urinary bladder walls, liver, and kidney were markedly inhibited with *P. dulce* administration. Further, we observed significant alterations in in situ formation or release of granulocyte-macrophage colony-stimulation factor (GM-CSF) and interferon gamma (IFN γ) in the *P. dulce* treated group compared with cyclophosphamide control group. The outcome of the study could have wide range of applications in combating chemotherapy-associated malnutrition as well as in cancer drug development.

Practical applications

CTX is a commonly used broad spectrum chemotherapeutic drug with severe side effects including immune suppression, malnutrition, urotoxicity, and nephrotoxicity. Identification of a novel immunomodulator from natural sources can resolve these side effects and could improve the quality of life of cancer patients receiving CTX as chemotherapeutic drug. In the present study, we had proved that *P. dulce* administration could significantly reduce CTX-induced immunotoxicity, urothelial toxicity, and nephrotoxicity. Administration of *P. dulce* showed a pronounced improvement in total leukocyte count, bone marrow cellularity/ α -esterase activity, expression of antioxidant glutathione and cytokines (GM-CSF and INF- γ) compared to CTX-treated mice group. Further, histopathological analysis confirmed the protective efficacy of *P. dulce* against CTX-induced urothelial, hepato and kidney damage. These insights are fostering new combinational therapeutic approaches to cancer treatment.

KEYWORDS

cyclophosphamide-induced immune suppression, granulocyte-macrophage colony-stimulating factor, immunomodulation, interferon gamma, *Pithecellobium dulce*, urotoxicity

1 | INTRODUCTION

Pithecellobium dulce (Roxb) Benth (Fabaceae) is medium-sized, spiny, evergreen tree that grows throughout the plains of India. Fruits of *P. dulce* have been used as food for a long time. Fruit aril of *P. dulce* is a dense source of thiamine, vitamin c, pectin, calcium, phosphorous, and iron. It is generally regarded as rich source of tannins, flavanoids, phenolics, and saponins and has shown to possess several vital biological properties such as antioxidant, anti-inflammatory, antidiarrheal, and antidiabetic property (Ponmozhi, Geetha, Saravana Kumar, & Suganya devi, 2011). HPLC analysis revealed the presence of phenolic and flavanoid components such as naringenin, quercetin, rutin, mandelic acid, gallic acid, elagic acid, and kaemferol (Megala & Geetha, 2010) from fruit arils of *P. dulce*. Anthocyanin, triterpene, n-malonyl-tryptophan, water soluble polysaccharides (PDP-1, PDP-2 and PDP-3), and saponins isolated from fruit arils of *P. dulce* are shown to exhibit several potential health benefits such as glucosidase inhibitory, antiparasitic, antioxidant, and antihyperglycemic activities (Kumar, Govindrajana, & Nyola, 2017; López-Angulo et al., 2018, 2019; Preethi & Saral, 2016; Sahu & Mahato, 1994). Hence it can be utilized as excellent source of natural antioxidants and can be considered as a functional food.

Cancer treatment-associated malnutrition is a massive long-standing root cause of health problem. Clearly, there exists an urgent need to adjure attention in these unforeseen nutritional problems and in producing highly nutritious food with highly medicinal value to attain optimal health and to power up immune system. The current issue with chemotherapeutic drugs is their toxic side effects to normal cells that adversely affect the quality of patient's life, regardless of their curative effects. Hence, embarked on a quest for the development of a curative counterfeit from natural sources with little adverse effect. Cyclophosphamide (CTX) is a widely used chemotherapeutic drug used to treat a variety of cancers. It is an alkylating agent with a high therapeutic index (Pass et al., 2005). CTX has potent antitumor effect with immunosuppression and cytotoxic effects (Singh, Gupta, Shau, & Ray, 1993). Combination therapy with protective agents can enhance the efficacy of anticancer drugs, reduce toxicity and also manage with the nutritional problem induced by these chemotherapeutic agents. In the ancient systems of medicine such as ayurveda and unani, concept of immunomodulation prevailed in order to alleviate diseases. In these systems, plants have been widely used to promote health and potentiate resistance against infections by modulating immune responses. CTX is being used in combination with several traditional medicinal herbs such as *Andrographis paniculata* (Sheeja & Kuttan, 2006), *Cassia occidentalis* (Bin-Hafeez, Ahmad, Haque, & Raisuddin, 2001), *Phyllanthus amarus* (Kumar, Banu, Kannan, & Pandian, 2005), etc. Such a dynamic systemic approach often limits the toxic complexity induced by chemical chemotherapeutic agents and provides promising outcomes of interest.

Despite the popular use of *P. dulce* fruits in various traditional medications including gastric problems, there are no scientific data available in in-vivo immunomodulatory effects. Hence prime approach of this work is to explore the protective effects of

Highlights

- The chemotherapeutic drug cyclophosphamide is found to induce immunosuppression, nephrotoxicity and urotoxicity.
- Combinational therapy with fruit extract of *Pithecellobium dulce* reduces the undesirable side effects of cyclophosphamide
- Treatment with fruit extract of *P. dulce* enhanced the levels of granulocyte-macrophage colony-stimulating factor (GM-CSF) and interferon gamma (IF- γ).

hydroalcoholic extract of *P. dulce*, which may strongly supports conventional chemotherapy in cancer treatments.

2 | MATERIALS AND METHODS

2.1 | Drugs and chemicals

Cyclophosphamide (CTX) was obtained from GLS Pharma Ltd. (Hyderabad, India). Gum acacia, Pararosaniline and 2-naphthyl acetate were purchased from Hi-Media (Mumbai, India). Harris hematoxylin was purchased from Spectrum Reagents and Chemicals Pvt. Ltd. (Kerala, India). MESNA was purchased from Cipla (Mumbai, India). GSH and 5-5 dithiobis-2-nitrobenzoic acid (DTNB; Ellmans reagent) were purchased from Molecular Probes Life Technologies (USA). Drabkin's reagent was procured from Agappe Diagnostics Ltd. (Kerala, India). Urea, creatinine, SGOT (serum glutamic oxaloacetic transaminase), SGPT (serum glutamate-pyruvate transaminase), and ALP (alkaline phosphatase) analyzing kits were purchased from Coral Clinical Systems (Goa, India). IFN- γ and GM-CSF ELISA kits were purchased from Peprotech (Rocky Hill, USA). All other chemicals used for experimental work were of analytical reagent grade.

2.2 | Animals

Female Balb/c mice (6–8 weeks old; 22–25 g) were purchased from Sree Chitra Tirunal Institute for Medical Sciences and Technology, Thiruvananthapuram. Animals were acclimatized for a period of one month prior to the study. The experimental animals were housed under well-ventilated polypropylene cages with controlled environmental condition maintained at a constant temperature ($25 \pm 2^\circ\text{C}$), 50% relative humidity, and 12-hr light/dark cycle. They were given rodent chow and tap water *ad libidum*. The study has been approved by Institutional Animal Ethics Committee (IAEC), Regional Cancer Centre, Thiruvananthapuram (IAEC/RCC NO. 4/17).

2.3 | Hydroalcoholic extraction of *P. dulce*

The fresh *P. dulce* fruits were collected from herbal garden centre for Indian Medicinal Heritage (CIMH), Kanjikode. The botanical identity

of collected plant specimen was confirmed by an eminent taxonomist and authenticated at Botanical Survey of India, Coimbatore (No: FAB/02/2018). A voucher specimen was deposited in herbarium of Division of Cancer Research, Regional Cancer Centre, Thiruvananthapuram.

Dried coarsely powdered fruit samples (20 g) were defatted with petroleum ether for 4 h. The defatted materials were then subsequently extracted with methanol and water (1:1) in a Soxhlet apparatus. The crude brown residue mass of extract was filtered through a 45- μ m filter and concentrated under reduced pressure using rotary vacuum evaporator and the percentage yield of the extract was 11% [w/w].

2.4 | Experimental design

Female Balb/c mice ($n = 90$) were divided into five groups ($n = 18$ /group). Group 1 served as normal group. Group 2 animals were administered with *P. dulce* extract (40 mg/kg B.Wt/po) for 10 consecutive days (Sakthivel & Guruvayoorappan, 2015). Groups 3, 4 and 5 were injected with CTX (25 mg/kg B.Wt/ip) for 10 consecutive days (Cui, Li, Wang, Su, & Xian, 2016; Feng et al., 2016; Sakthivel & Guruvayoorappan, 2015). Group 3 served as CTX control group. Groups 4 and 5 were administered with MESNA (25 mg/kg B.Wt/ip) (Cui et al., 2016; Feng et al., 2016; Sakthivel & Guruvayoorappan, 2015) and *P. dulce* extract (40 mg/kg B.Wt/op) respectively for 10 consecutive days starting from the same day of CTX administration (Figure 1). The animals were sacrificed on Day 7 ($n = 6$) and Day 11 ($n = 6$) by cervical dislocation. Blood was collected by cardiac puncture and used for analyzing hematological parameters. Serum separated was used for estimating biochemical parameters and cytokine profile. The vital organs (spleen, liver, kidney, thymus, and lungs), bone marrow, and the urinary bladder were dissected out and washed with phosphate-buffered saline (pH-7.4).

Macroscopic examinations of the organs were performed using blind study. The tissues were homogenized using homogenizing buffer (Tris buffer [pH 7.4]) and the homogenates were used for studying biochemical parameters. A portion of the tissue was fixed in formaldehyde (10%) and subjected to histopathological studies.

2.4.1 | Acute and subacute toxicity studies

Acute and subacute in vivo toxicity study of *P. dulce* extract has been carried out as per Organization for Economic Co-operation and Development guidelines 423 and 407. In acute in vivo toxicity study, the *P. dulce* extract has been administered orally in escalating doses (100 mg/kg up to 2,000 mg/kg). The general behaviors such as aggressiveness, autonomic or behavioral responses, tremors, convulsions, consumption rate of food, body weight, sedation, changes in mucous membrane, mydriasis, diarrhea, lacrimation, rising of fur, coma were continuously observed for 4 hr. Rate of mortality was also determined. Animals were observed at least once during the first 30 min, periodically during the first 24 hr, with special attention given during the first 4 hr and daily thereafter for a period of 14 days. In subacute toxicity study, the different fractions (1/5, 1/10, and 1/20 of LD50) of tested *P. dulce* extract were administered orally (op) for a period of 28 days. The body weights of all animals were measured during the period of acclimatization, once before the commencement of dosing and once on the day of sacrifice. All animals were monitored daily for clinical signs and mortality patterns once before dosing and up to 4 hr after dosing (Al-Mamary, Al-Habori, Al-Aghbaria, & Baker, 2002). On Day 29, animals were sacrificed and relative organ weight, hematological and serum biochemical parameters were evaluated.

2.4.2 | Hematological parameter and body weight

For this study, a batch of 30 mice (6 per group) received the same treatment as described in the experimental session. The change in average body weights of animals were recorded every 3rd day for 30 days. The blood was collected from each animal by tail vein bleeding on every third day and continued for 30 days. Hematological parameters such as total leukocyte count (TLC) and hemoglobin content were determined.

2.4.3 | Relative organ weight, bone marrow cellularity, and alpha esterase activity

Animals were divided into five groups ($n = 12$ /group) and received the same treatment as described in the experimental session. Six

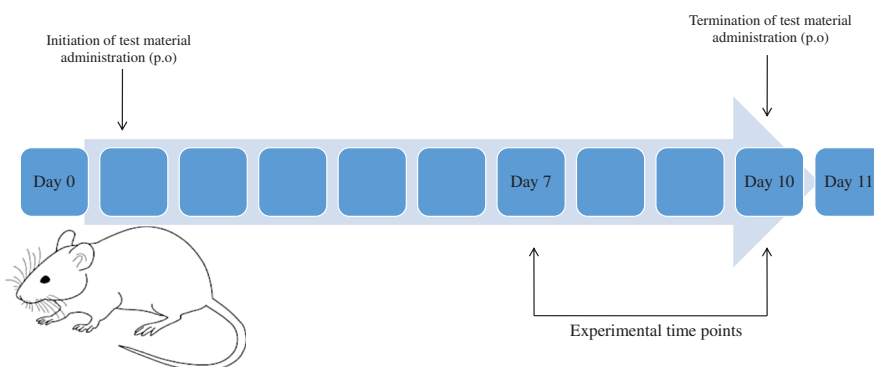


FIGURE 1 Schematic representation showing the general time course of study

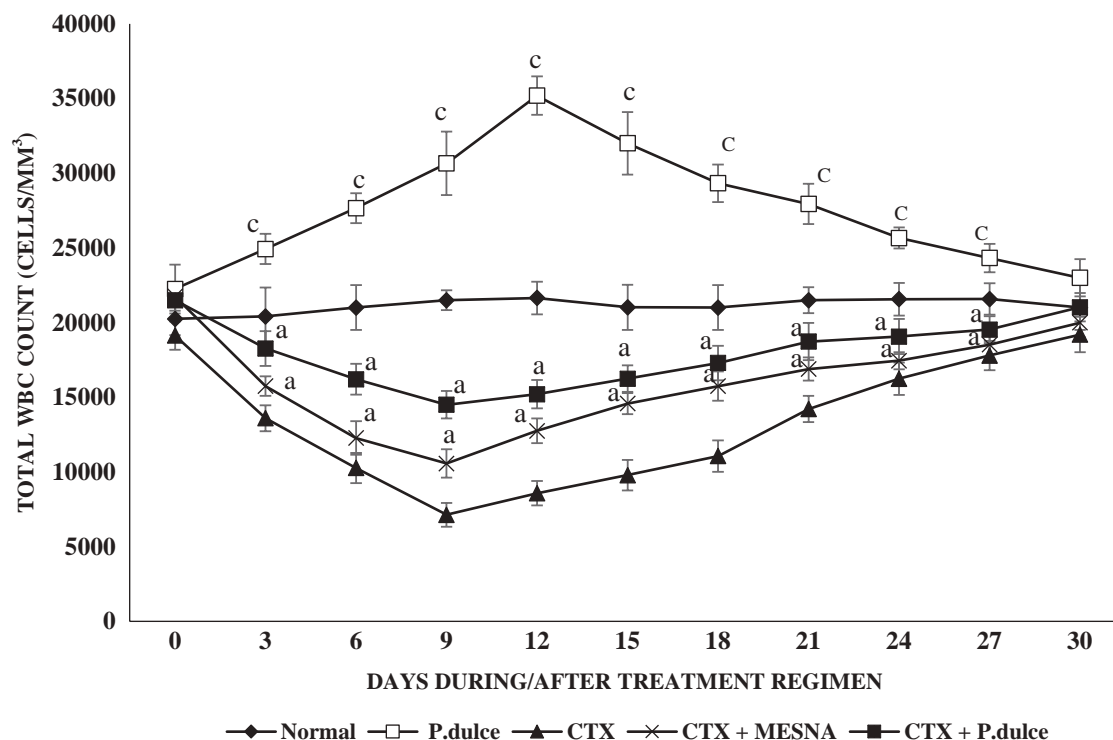


FIGURE 2 Summarize the effects on total leukocyte count in mice at different time points. All treatments were given a total of 10 consecutive days; every third day (starting from Day 0 (prior to first treatment)) blood was collected by tail vein method and total leukocyte counts were measured. Statistical analysis was performed and values are expressed as mean \pm standard deviation (SD). ^a $p < .01$ for CTX alone versus CTX + extract or CTX + MESNA co-treated, ^c $p < .01$ for *P. dulce* extract alone versus normal animal

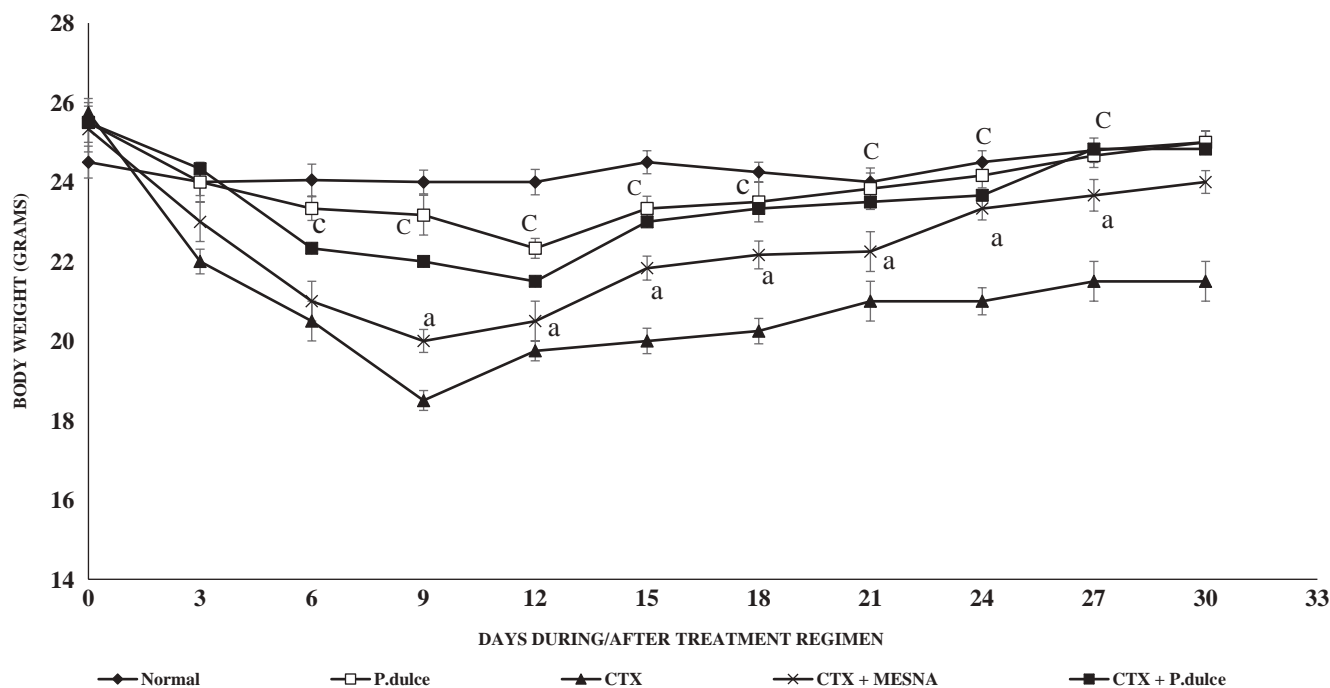


FIGURE 3 Effect of *P. dulce* on the body weight of animals during CTX-induced immunosuppression: Summarizes the effect of treatments on body weight of mice at course of study. All treatments were given a total of 10 consecutive days; every third day (starting from Day 0 (prior to first treatment)). Body weight of each animal was measured and statistical analysis was performed. All values are expressed as mean \pm standard deviation (SD). ^a $p < .01$, for CTX alone versus CTX + extract or CTX + MESNA co-treated, ^c $p < .01$, for *P. dulce* extract alone versus normal animal

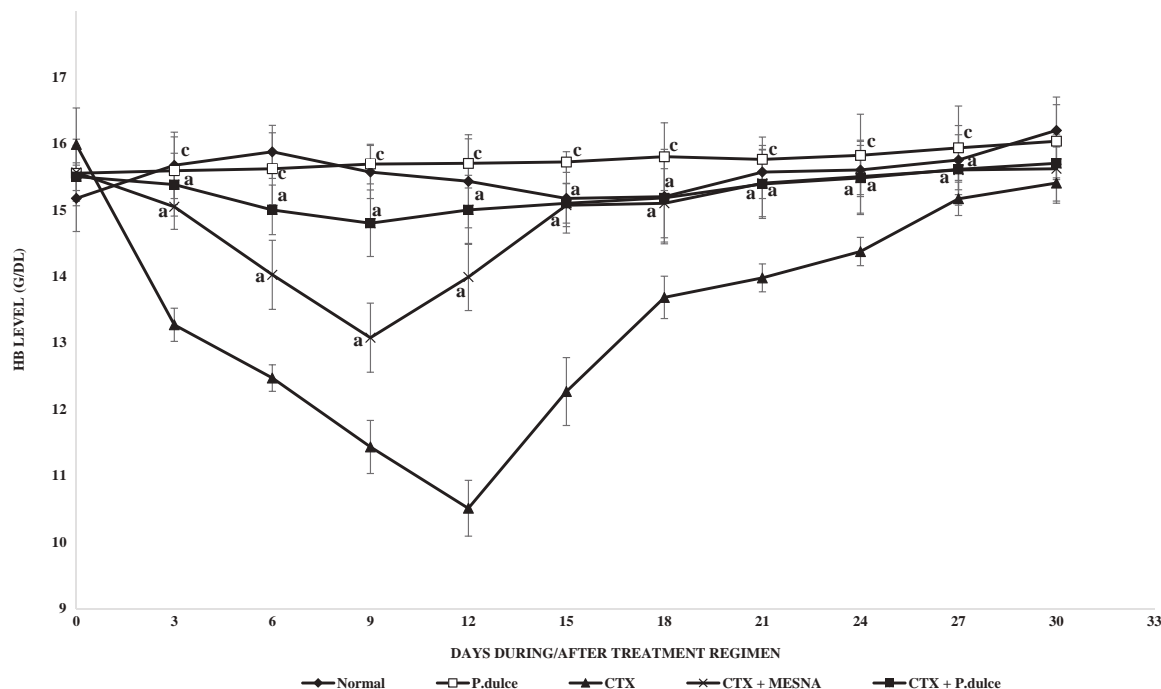


FIGURE 4 Effect of *P. dulce* on the hemoglobin level during CTX-induced immunosuppression: Summarizes the effect of treatments on hemoglobin (Hb) in mice at different time points. All treatments were given a total of 10 consecutive days; every third day (starting from Day 0 (prior to first treatment)) blood was collected by tail vein method and Hb level was measured. Statistical analysis was performed using one way ANOVA. All values are expressed as mean \pm SD. ^a $p < .01$, for CTX alone versus CTX + extract or CTX + MESNA co-treated, ^c $p < .01$, for *P. dulce* extract alone versus normal animal

animals from each group were euthanized on Day 7 and Day 11. The thymus, spleen, lungs, liver, kidney, and urinary bladder were excised immediately, washed thoroughly with ice cold saline, gently blotted, and weighed. Femurs were then perfused using PBS by inserting syringe through medullary cavity. Bone marrow cells were collected and mixed thoroughly for obtaining single cell suspension. The number of α -esterase positive cells was assessed by azo dye coupling method as described by Bancroft and Cook (1994) and results were expressed in number of positive cells/4,000 bone marrow cells.

2.4.4 | Analysis of biochemical parameters and cytokine profiling

Serum from the aforementioned experiment was used to estimate different serum markers and cytokine analysis. Serum markers including urea, creatinine, serum glutamic-oxaloacetic transaminase (SGOT), serum glutamic-pyruvic transaminase (SGPT), and alkaline phosphatase (ALP) were analyzed via commercial diagnostic kit as per manufacture's instruction (Coral Clinical Systems). Urinary bladder, kidney, and portion of small intestine were homogenized in 10% (w/v) ice cold 0.1 M Tris buffer (pH 7.4) using homogenizer and the resulting homogenate was used to determine total reduced glutathione (GSH) and lipid peroxidation (LPO) content (Ohkawa, Ohishi, & Yagi, 1979).

The levels of proinflammatory cytokines such as IFN- γ and GM-CSF were analyzed using ELISA kit from Peprotech (Rocky Hill, USA).

In all cases, the experiments were performed as per manufacture's instructions.

2.4.5 | Histopathological examination

A portion of urinary bladder, kidney, and liver tissue sample from each mouse was collected and fixed in 10% formaldehyde solution. The preserved samples were then processed for routine paraffine wax block preparation using an optical rotary microtome. Sections of 4 μ m were prepared, stained using H&E (hematoxylin and eosin) and examined under microscope (40 \times magnification).

2.4.6 | Statistical analysis

Values were expressed as mean \pm standard deviation. The group means were compared using a one-way analysis of variance (ANOVA) followed by Dunnett's test using instat version 3.0 software (Graphpad, San Diego, CA). $p < .05$ was considered to be statistically significant.

3 | RESULTS

3.1 | Acute and subacute toxicity studies

The extract seems to be safe and non-toxic at a dose level of 40 mg/kg B.wt *P. dulce*. No major changes in general behaviors (aggressiveness, autonomic or behavioral responses, tremors, convulsions,

consumption rate of food, body weight, sedation, changes in mucous membrane, mydriasis, diarrhea, lacrimation, rising of fur, coma) and mortality were observed (data not shown). Administration of 2,000 mg/kg B.wt did not show any signs of toxicity or mortality during the entire observation period. Hence this data suggests that *P. dulce* extract is non-toxic in single dose of 2,000 mg/kg B.wt. Therefore, LD₅₀ of *P. dulce* extract could be considered as 2,000 mg/kg B.wt. In subacute toxicity study, the relative organ weight of vital organs, hematological, and serum biochemical parameters was analyzed (data not shown). No significant changes were observed in all groups. Based on these data, it was found that the dose at a concentration of 40 mg/kg B.wt was selected for performing the experiments.

3.2 | Hematological parameters and body weight

The effect of different treatments on TLC is depicted in Figure 2. The treatment with CTX reduced the TLC and the maximal impact of CTX was observed on Day 9 of the treatment period. On Day 9, CTX administrated group exhibited a TLC of only 7,133 [±800.42]/mm³ compared to normal 21,500[±661]/mm³. On contrary, blood samples from the co-treated group (*P. dulce* + CTX) showed a significant improvement in TLC (14,500 [±924.64]/mm³) compared to CTX alone group (7,133 [±800.42]/mm³). *P. dulce* extract administrated group showed a very high TLC 30,666 [±2,119]/mm³ compared to normal mice (21,500[±661]/mm³).

Effects on body weight are shown in Figure 3. The CTX administrated group (18.5[±0.25] g) showed a significant reduction in body weight (similar to the aforementioned observation) relative to normal group (24 [±0.30] g). However, the co-treatment of extract along with CTX elevates the reduced level to 22[±0.25] g.

The effects on hemoglobin content are presented in Figure 4. Treatment with CTX significantly decreased the hemoglobin content 10.5% [±0.42] gm %, and maximal hemoglobin content dip was observed on Day 12 of the treatment period. While co-treated group showed a statistically significant improvement in hemoglobin content 15% [±0.7] gm % compared to CTX alone group (10.5% [±0.42] gm %). No significant changes were observed in hemoglobin content after administration of *P. dulce* extract 15% [±0.3] gm % compared to normal mice 15% [±0.7] gm %.

3.3 | Effect on relative organ weight, bone marrow cellularity, and α-esterase activity

Relative organ weights of spleen, liver, kidney, thymus, lungs, and urinary bladder on Day 7 and Day 11 are depicted in Table 1. The weight of spleen, thymus, and liver was significantly elevated by administration of *P. dulce* extract compared to normal group. Furthermore, treatment with CTX significantly reduced relative organ weight of spleen, thymus, and liver compared to normal group. Moreover, these changes were reversed after co-administration of extract with CTX. CTX treatment caused a significant increase in relative weight of kidney and urinary bladder compared with normal group but this

TABLE 1 Effect of *P. dulce* on the relative organ weight during CTX-induced immunosuppression

Treatment	Relative organ weights (g/100 g BW)									
	Spleen		Thymus		Liver		Kidney		Lungs	
	Day 7	Day 11	Day 7	Day 11	Day 7	Day 11	Day 7	Day 11	Day 7	Day 11
Normal	0.29 ± 0.02	0.32 ± 0.04	0.14 ± 0.01	0.14 ± 0.03	5.95 ± 0.7	6.25 ± 0.21	1.65 ± 0.07	1.68 ± 0.06	0.67 ± 0.04	0.67 ± 0.05
<i>P. dulce</i>	0.67 ± 0.05 ^c	0.87 ± 0.20 ^c	0.14 ± 0.01	0.17 ± 0.01	6.35 ± 0.49 ^d	6.56 ± 0.49 ^d	1.6 ± 0.08	1.7 ± 0.07	0.64 ± 0.01	0.65 ± 0.01
CTX	0.23 ± 0.030	0.25 ± 0.01	0.09 ± 0.01	0.06 ± 0.02	5.9 ± 0.14	5.85 ± 0.07	2.02 ± 0.07	2.06 ± 0.08	0.52 ± 0.01	0.61 ± 0.01
CTX + MESNA	0.36 ± 0.03 ^b	0.4 ± 0.01 ^a	0.10 ± 0.01 ^a	0.09 ± 0.01 ^b	6.25 ± 0.14 ^a	5.94 ± 0.12 ^b	2 ± 0.07	1.9 ± 0.04	0.66 ± 0.01 ^a	0.67 ± 0.02 ^a
CTX + <i>P. dulce</i>	0.42 ± 0.06 ^a	0.47 ± 0.07 ^a	0.10 ± 0.01 ^a	0.14 ± 0.01 ^a	7.73 ± 0.15 ^a	6.19 ± 0.13 ^a	1.8 ± 0.07	1.88 ± 0.09	0.69 ± 0.02 ^a	0.70 ± 0.08 ^a
									0.05 ± 0.01 ^a	0.07 ± 0.01 ^a

Note: Statistical analysis was performed using one way ANOVA. All values are expressed as mean ± SD. ^a*p* < .01, ^b*p* < .01 for CTX alone versus CTX + extract or CTX + MESNA co-treated, ^c*p* < .01, ^d*p* < .01 for *P. dulce* extract alone versus normal animal.

TABLE 2 Effect of *P. dulce* on bone marrow cellularity and α -esterase activity during CTX-induced immunosuppression

Treatment groups	Bone marrow cellularity (cells/femur)		α -esterase activity (esterase ⁺ cells/4,000 cells)	
	Day 7($\times 10^6$)	Day 11($\times 10^6$)	Day 7	Day 11
Normal	$155 \times 10^5 \pm 3.12$	$150.2 \times 10^5 \pm 6.8$	833 ± 13.4	848 ± 14
<i>P. dulce</i>	$184 \times 10^5 \pm 4.9^d$	$228.0 \times 10^5 \pm 9.8^c$	$1,170 \pm 14.1^c$	$1,271 \pm 55.2^c$
CTX	$56.5 \times 10^5 \pm 3.5^{b,a}$	$75.0 \times 10^5 \pm 6.0^{a,a}$	$566 \pm 62^{a,a}$	$579 \pm 33.2^{a,a}$
CTX + MESNA	$118 \times 10^5 \pm 19.1^a$	$134 \times 10^5 \pm 19^a$	770 ± 25.5^a	805 ± 9.9^a
CTX + <i>P. dulce</i>	$75 \times 10^5 \pm 9.5^b$	$127 \times 10^5 \pm 10.3^a$	739 ± 12.7^a	815 ± 7.1^a

Note: Statistical analysis was performed using one way ANOVA. All values are expressed as mean \pm SD. ^a $p < 0.01$, ^b $p < 0.01$ for CTX alone versus CTX/extract or CTX/MESNA co-treated, ^c $p < 0.01$, ^d $p < 0.01$ for *P. dulce* extract alone versus normal animal.

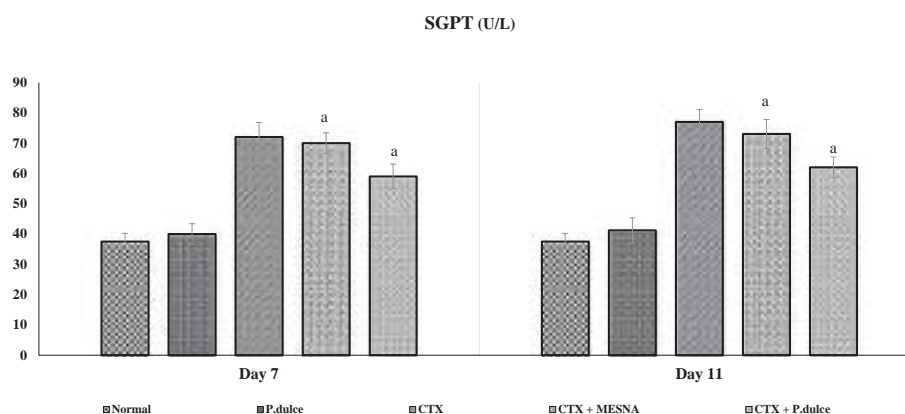


FIGURE 5 Effect of *P. dulce* on the serum SGPT level during CTX-induced immunosuppression: CTX (25 mg/kg B.Wt/ip) were administered intraperitoneally for 10 consecutive days. Simultaneously, 50 mg/kg B.Wt/ip. *P. dulce* extract was injected for 10 consecutive days. Blood was collected on Day 7 and Day 11. Serum SGPT levels were measured using commercial diagnostic kits. Statistical analysis was performed using one way ANOVA. All values are expressed as mean \pm SD. ^a $p < .01$ for CTX alone versus CTX + extract or CTX + MESNA co-treated

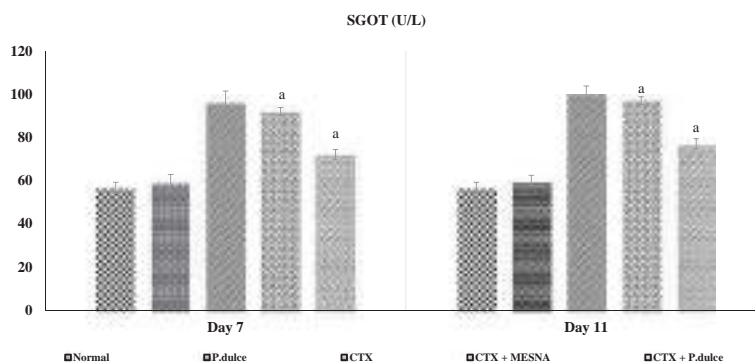


FIGURE 6 Effect of *P. dulce* on the serum SGOT level during CTX-induced immunosuppression: All values are expressed as mean \pm SD. ^a $p < .01$ for CTX alone versus CTX + extract or CTX + MESNA co-treated

was reversed by administration of CTX with extract (CTX + *P. dulce*) and CTX along with MESNA (CTX + MESNA). No apparent changes could be evidenced in relative weight of lungs during any course of treatment.

The effect of *P. dulce* treatments on bone marrow cellularity and α -esterase activity is depicted in Table 2. The bone marrow cellularity and α -esterase positive cells were reduced drastically in CTX treated group (on both Day 7 and Day 11) compared to normal. As in the previous experiment, this was significantly reversed upon co-treatment with *P. dulce* along with CTX.

3.4 | Effect on serum hepatic toxicity marker enzymes

Effect of *P. dulce* treatment on serum SGPT, SGOT, and ALP levels is depicted in Figures 5–7. Administration of CTX significantly induced serum SGPT, SGOT, and ALP on Day 7 and Day 11 compared to normal. However, co-treatment with *P. dulce* extract markedly decreased serum SGPT, SGOT and ALP levels compared to CTX alone group on both day 7 and day 11. In contrast, in extract alone treated groups, those values were in the same range as in the normal group.

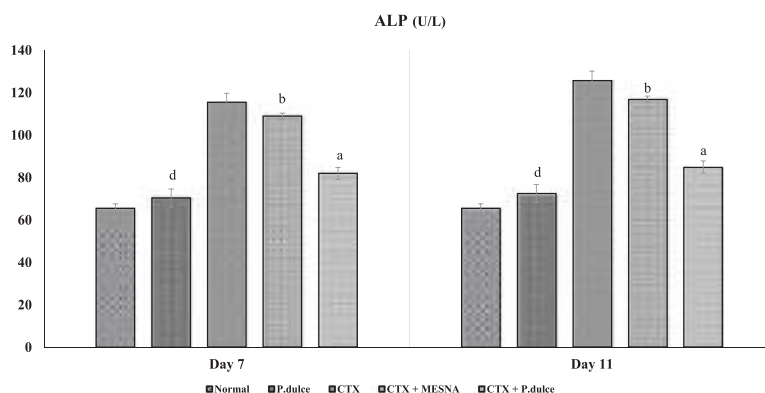


FIGURE 7 Effect of *P. dulce* on the serum ALP level during CTX-induced immunosuppression. All values were expressed as mean \pm SD. ^a $p < .01$, ^b $p < .05$ for CTX alone versus CTX + extract or CTX + MESNA co-treated, ^d $p < .05$ for *P. dulce* extract alone versus normal animal

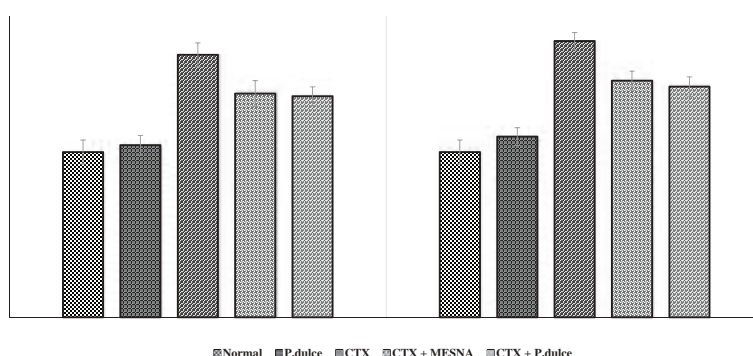


FIGURE 8 Effect of *P. dulce* on the serum urea level during CTX-induced immunosuppression. All values were expressed as mean \pm SD. ^a $p < .01$ for CTX alone versus CTX + extract or CTX + MESNA co-treated

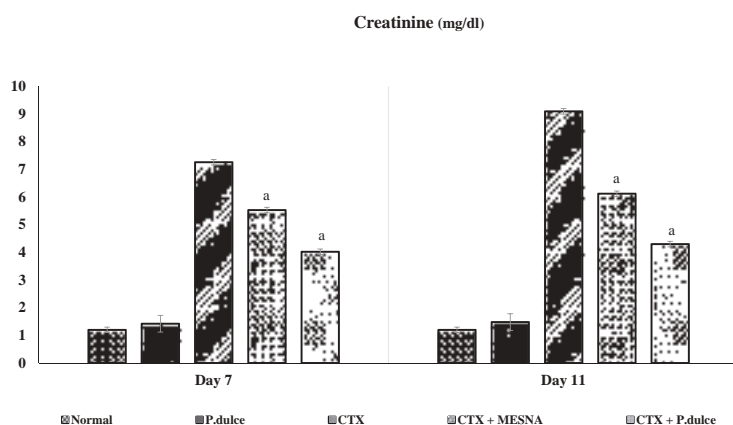


FIGURE 9 Effect of *P. dulce* on the serum creatinine level during CTX-induced immunosuppression. All values are expressed as mean \pm SD. ^a $p < .01$ for CTX alone versus CTX + extract or CTX + MESNA co-treated

3.5 | Effect on serum renal toxicity marker enzymes

Effect of *P. dulce* treatment on serum urea and creatinine is depicted in Figures 8 and 9. Administration of CTX significantly induced serum urea and creatinine on Day 7 and Day 11 compared to normal. However, co-treatment with *P. dulce* extract significantly reduced serum urea and creatinine levels on day 7 and day 11 when compared to CTX alone group. In contrast, in extract alone treated groups, those values were in the same range as in the normal group.

3.6 | Effect of treatments on bladder LPO and GSH levels

The effect of treatments on bladder GSH and LPO levels is presented in Table 3. Due to CTX, LPO elevated up to 6.02 [± 0.5] and 6.4 [± 0.3] nmoles/mg protein were observed on day 7 and day 11 respectively, while normal values were just 1.98 [± 0.2] and 2.0 [± 0.3] nmoles/mg protein. Co-treatments with extract (2.90 [± 0.2] and 3.8 [± 0.1] nmoles/mg protein respectively) or MESNA (2.10 [± 0.3] and 3.0 [± 0.1]

TABLE 3 Effect of *P. dulce* on urinary bladder lipid peroxidation and GSH levels during CTX-induced immunosuppression

	Lipid peroxidation (nmoles/mg protein)		GSH (nmoles/mg protein)	
	Urinary bladder		Urinary bladder	
	Day 7	Day 11	Day 7	Day 11
Normal	1.98 ± 0.2	2.0 ± 0.3	18.50 ± 0.7	20.3 ± 0.4
<i>P. dulce</i>	2.00 ± 0.2 ^c	2.5 ± 0.2 ^c	16.80 ± 0.1 ^c	17.6 ± 0.1 ^c
CTX	6.02 ± 0.5 ^{a,a}	6.4 ± 0.3 ^{a,a}	8.75 ± 0.1 ^{a,a}	9.85 ± 0.1 ^{a,a}
CTX + MESNA	2.10 ± 0.3 ^a	3.0 ± 0.1 ^a	13.40 ± 0.1 ^a	13.6 ± 0.3 ^a
CTX + <i>P. dulce</i>	2.90 ± 0.2 ^a	3.8 ± 0.1 ^a	13.15 ± 0.1 ^a	14.0 ± 0.3 ^a

Note: All values are expressed as mean ± SD. ^a*p* < .01 for CTX alone versus CTX + extract or CTX + MESNA co-treated, ^c*p* < .01 for *P. dulce* extract alone versus normal animal.

TABLE 4 Effect of *P. dulce* on intestinal lipid peroxidation and GSH levels during CTX-induced immunosuppression

	Lipid peroxidation (nmoles/mg protein)		GSH (nmoles/mg protein)	
	Small intestine		Small intestine	
	Day 7	Day 11	Day 7	Day 11
Normal	1.60 ± 0.1	1.8 ± 0.2	6.00 ± 0.3	6.10 ± 0.2
<i>P. dulce</i>	2.30 ± 0.2 ^c	2.5 ± 0.2 ^c	5.30 ± 0.3 ^c	5.90 ± 0.1 ^c
CTX	4.60 ± 0.3 ^{a,a}	4.8 ± 0.4 ^{a,a}	4.45 ± 0.1 ^{a,a}	4.55 ± 0.2 ^{a,a}
CTX + MESNA	3.70 ± 0.2 ^a	4.0 ± 0.1 ^a	5.65 ± 0.2 ^a	6.10 ± 0.6 ^a
CTX + <i>P. dulce</i>	2.95 ± 0.2 ^a	3.0 ± 0.1 ^a	5.30 ± 0.3 ^a	5.90 ± 0.1 ^a

Note: All values are expressed as mean ± SD. ^a*p* < .01 for CTX alone versus CTX + extract or CTX + MESNA co-treated, ^c*p* < .01 for *P. dulce* extract alone versus normal animal.

TABLE 5 Effect of *P. dulce* on kidney lipid peroxidation and GSH levels during CTX-induced immunosuppression

	Lipid peroxidation (nmoles/mg protein)		GSH (nmoles/mg protein)	
	Kidney		Kidney	
	Day 7	Day 11	Day 7	Day 11
Normal	1.9 ± 0.15	1.6 ± 0.60	45 ± 6.0	47 ± 4.5
<i>P. dulce</i>	3.4 ± 0.36 ^c	3.9 ± 0.10 ^c	38 ± 5.5 ^c	41 ± 6.1 ^c
CTX	3.7 ± 0.50 ^{a,a}	4.3 ± 0.47 ^{a,a}	26 ± 5.6 ^{a,a}	27 ± 4.1 ^{a,a}
CTX + MESNA	2.2 ± 0.10 ^a	2.0 ± 0.20 ^a	26 ± 4.1 ^a	29 ± 4.0 ^a
CTX + <i>P. dulce</i>	2.7 ± 0.21 ^a	2.8 ± 0.15 ^a	32 ± 5.5 ^a	34 ± 5.0 ^a

Note: All values are expressed as mean ± SD. ^a*p* < .01 for CTX alone versus CTX + extract or CTX + MESNA co-treated, ^c*p* < .01 for *P. dulce* extract alone versus normal animal.

nmoles/mg protein respectively) reversed these trends. In contrary, CTX treated group showed a significant decrease in GSH (8.75[±0.1] and 9.85[±0.1] nmoles/mg protein, respectively) compared to normal on both day 7 and day 11 (18.50[±0.7] and 20.3 [±0.4] nmoles/mg protein). However in co-treated group (CTX + *P. dulce*; 13.15[±0.1] and 14.0 [±0.3] nmoles/mg protein, respectively or CTX + MESNA; 13.40 [±0.1] and 13.6 [±0.3] nmol/mg protein, respectively), a significant increase in GSH was observed versus the CTX alone at both days (7th and 11th; 8.75[±0.1] and 9.85[±0.1] nmoles/mg protein, respectively). In contrast, in extract alone treated groups, those

values were almost same range as in the normal group (7th and 11th; 18.50[±0.7] and 20.3[±0.4] nmoles/mg protein, respectively).

3.7 | Effect of treatments on intestinal LPO and GSH levels

The effect of treatments on intestinal GSH and LPO level is presented in Table 4. Due to CTX, LPO elevated upto 4.60 [±0.3] and 4.8 [±0.4] nmoles/mg protein were observed on day 7 and day 11 respectively, while normal values were just 1.60 [±0.1] and 1.8 [±0.2] nmoles/

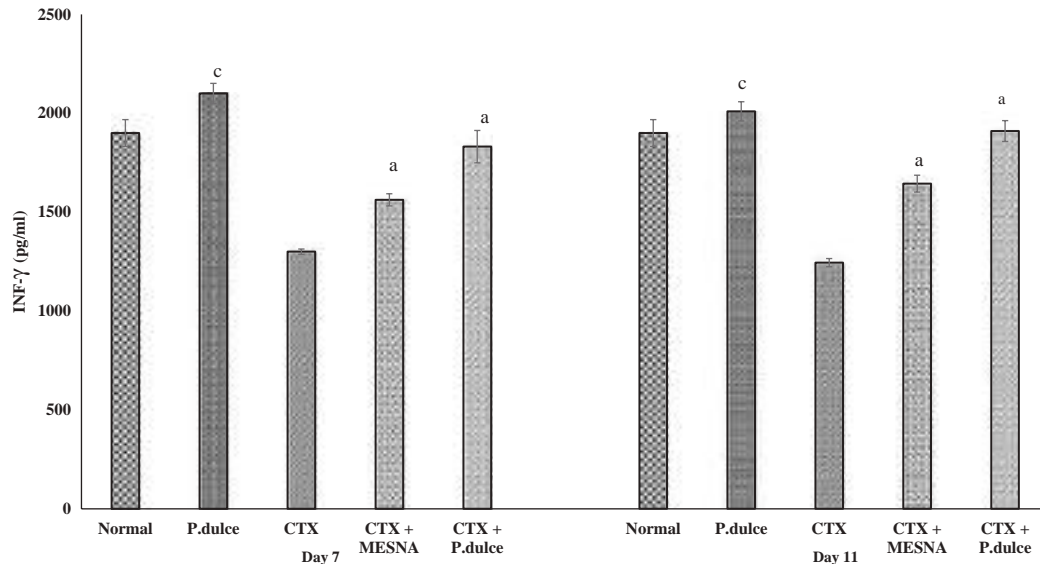


FIGURE 10 Effect of *P. dulcis* on the serum IFN γ level during CTX-induced immunosuppression. All values are expressed as mean \pm SD. ^a $p < .01$ for CTX alone versus CTX + extract or CTX + MESNA co-treated, ^c $p < .01$ *P. dulcis* extract alone versus normal animal

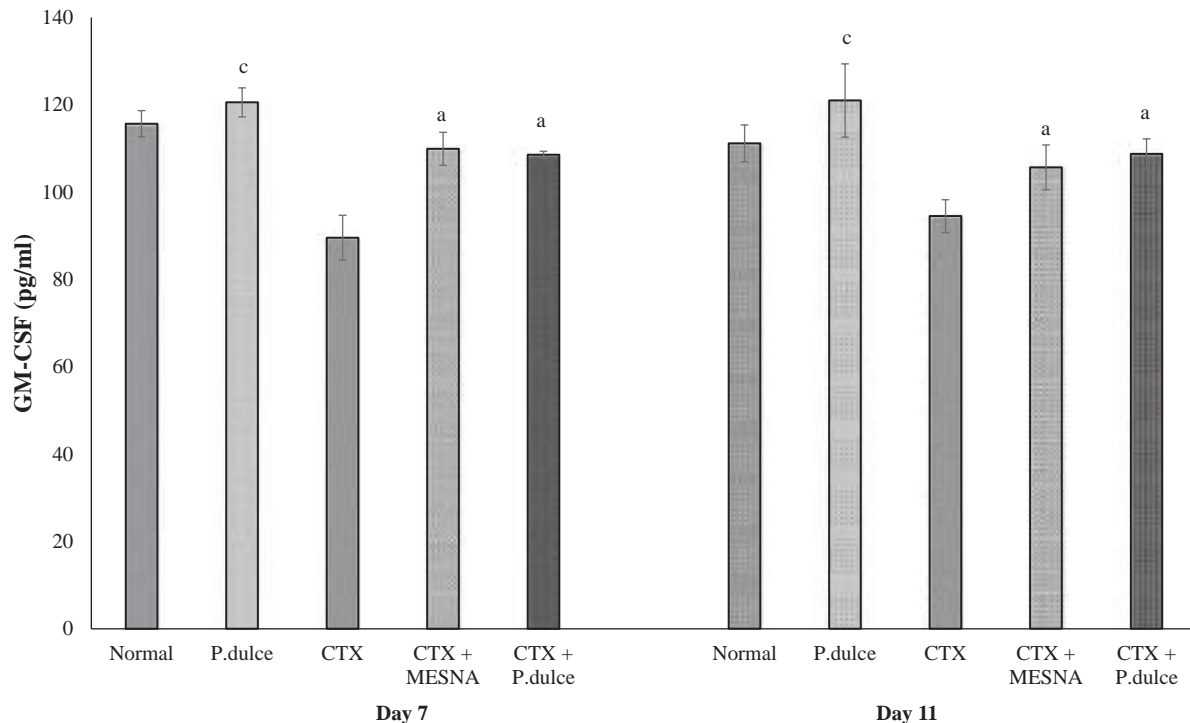


FIGURE 11 Effect of *P. dulcis* on the serum GM-CSF level during CTX-induced immunosuppression. All values are expressed as mean \pm SD. ^a $p < .01$ for CTX alone versus CTX + extract or CTX + MESNA co-treated, ^c $p < .01$ for *P. dulcis* extract alone versus normal animal

mg protein. Co-treatments with extract caused a significant reversal of this outcome (2.95 ± 0.2) and 3.0 ± 0.1 nmoles/mg protein). In contrary, CTX treated group showed a significant decrease in GSH (4.45 ± 0.1) and 4.55 ± 0.2 nmoles/mg protein) compared to normal (6.00 ± 0.3) and 6.10 ± 0.2 nmol/mg protein) on both day 7 and day 11. However, in co-treated group (CTX + *P. dulcis*) showed a significant increase in GSH (5.30 ± 0.3) and 5.90 ± 0.1 nmoles/mg protein) was observed versus the CTX alone at both days (7th and 11th; 4.45 ± 0.1) and 4.55 ± 0.2 nmoles/mg protein).

3.8 | Effects of treatments on kidney LPO and GSH levels

The effect of treatments on kidney GSH and LPO level is presented in Table 5. Due to CTX, LPO elevated up to 3.7 ± 0.50 and 4.3 ± 0.47 nmoles/mg protein was observed on Day 7 and Day 11, respectively, while normal values were just 1.9 ± 0.15 and 1.6 ± 0.60 nmoles/mg protein. Co-treatments with extract caused a significant reversal of this outcome (2.7 ± 0.21) and 2.8 ± 0.15 nmoles/mg protein). In

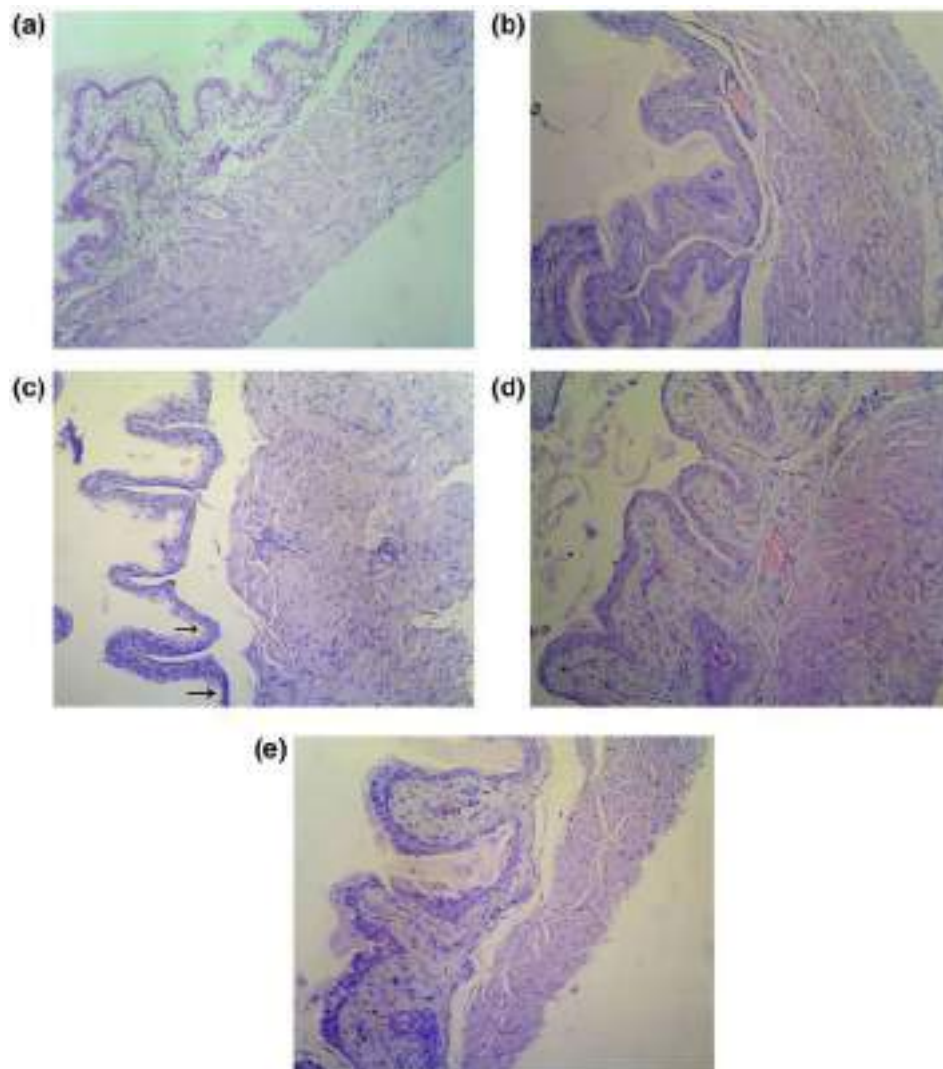


FIGURE 12 Effect of *P. dulce* on urinary bladder histology during CTX-induced immunosuppression. Photomicrograph of a mouse from each treatment regimen is represented here. (a) Section from normal mice. (b) Extract alone group. (c) CTX alone group. (d) CTX + MESNA group. (e) CTX + extract group. (Magnification—40 \times)

contrary, CTX treated group showed a significant decrease in GSH (26[\pm 5.6] and 27[\pm 4.1] nmoles/mg protein) compared to normal (45 [\pm 6.0] and 47 [\pm 4.5] nmoles/mg protein) on both Day 7 and Day 11. However, in co-treated group, a significant increase in GSH (32 [\pm 5.5] and 34 [\pm 5] nmoles/mg protein) was observed versus the CTX alone at both days (7th and 11th; 26 [\pm 5.6] and 27 [\pm 4.1] nmoles/mg protein).

3.9 | Effect on serum cytokine levels

Effects on serum IFN- γ and GM-CSF are depicted in Figures 10 and 11. Administration of CTX markedly decreased serum cytokine levels. Significant decrease of serum IFN- γ and GMCSF was seen around Day 7 (1,300.33 [\pm 13.4] or 89.56 [\pm 5.123] pg/ml, respectively) and Day 11 (1,244.7[\pm 20.82] and 94.53 [\pm 3.76] pg/ml, respectively) compared to naive control (1,900.15[\pm 68] and 115.67[\pm 3.34] pg/ml, respectively). Co-treatments with extract

caused a significant reversal of this outcome (Day 7; (1,831.5[\pm 82] or 108.565[\pm 8.04] pg/ml, respectively and Day 11; 1,910.52 [\pm 52.8] or 108.78 [\pm 3.45] pg/ml, respectively). Almost similar results were obtained for MESNA group (Day 7; 1,562.03[\pm 30.8] or 109.92[\pm 3.788] pg/ml, respectively and Day 11; 1,644 [\pm 42.5] or 105.663 [\pm 5.14] pg/ml, respectively). While mice that received only *P. dulce* extract showed a slight increase in serum IFN- γ and GM-CSF (Day 7; 2,100.12[\pm 51.2] or 120.57[\pm 3.34] pg/ml, respectively and Day 11; 2,010.05 [\pm 48.5] or 121[\pm 5.13] pg/ml, respectively) versus values seen in naive control (1,900.15[\pm 68] and 115.67[\pm 3.34] pg/ml, respectively).

3.10 | Histopathology

The effect of *P. dulce* extract on CTX-induced histopathological changes in urinary bladder, liver, and kidney is represented in Figures 12–14. The histological evaluation of bladder sample treated with

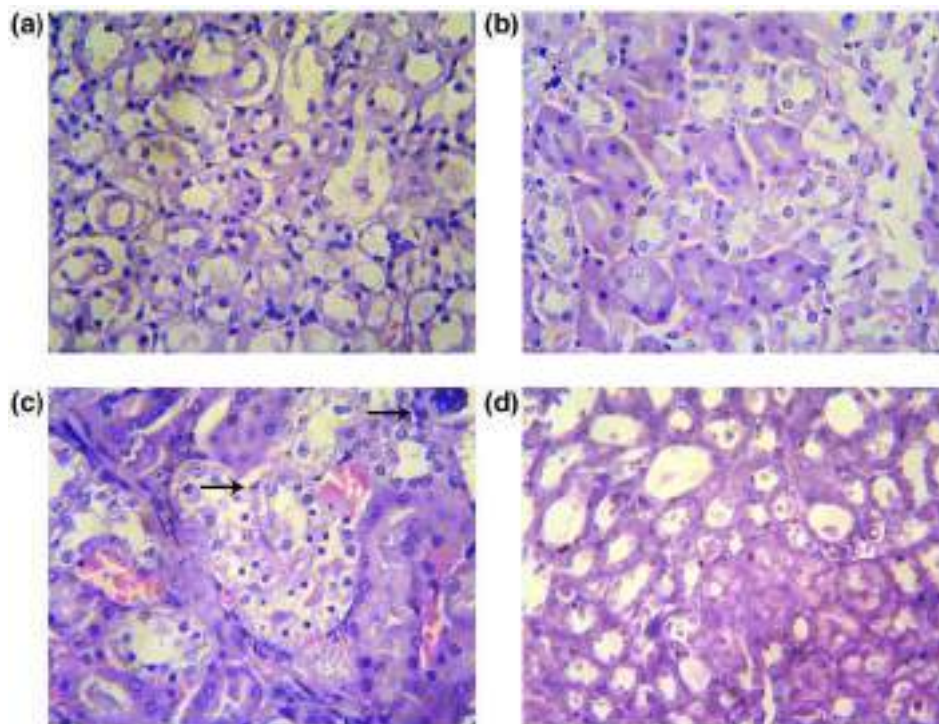


FIGURE 13 Effect of *P. dulce* on Kidney histology during CTX-induced immunosuppression. Photomicrograph of one mouse from each group is represented here. (a) Section from normal mice. (b) Extract alone group. (c) CTX alone group. (d) CTX + extract group. (Magnification—40×)

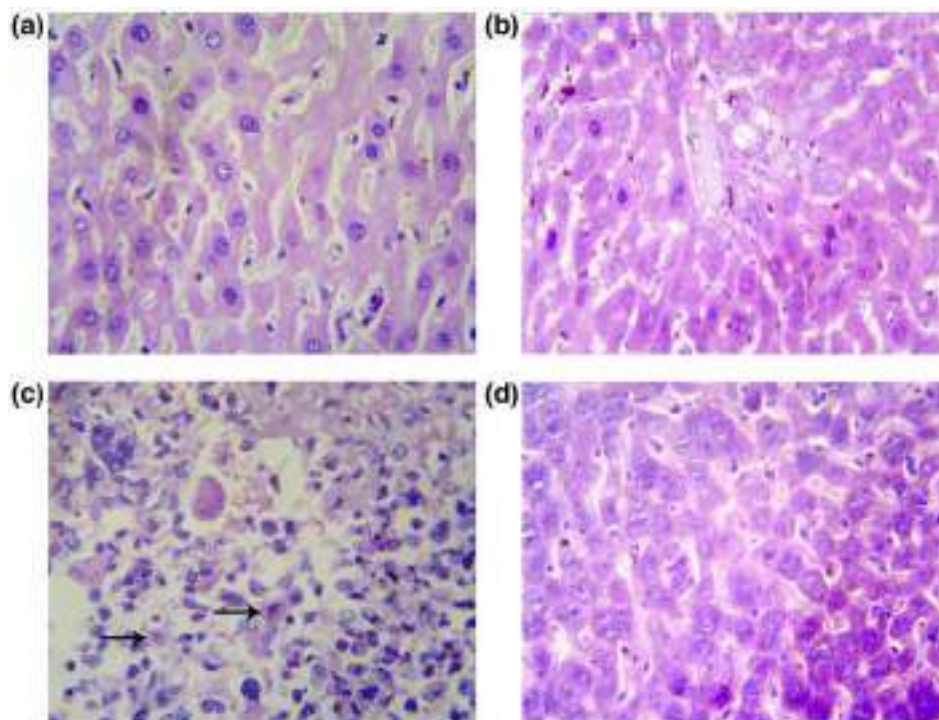


FIGURE 14 Effect of *P. dulce* on the liver histology during CTX-induced immunosuppression. Photomicrograph of a mouse from each treatment regimen is represented here. (a) Section from normal mice. (b) Extract alone group. (c) CTX alone group. (d) CTX + extract group. (Magnification—40×)

CTX showed severe damage of urothelium including inflammatory cell infiltration, vasodilation, mucosal erosion, fibrin deposition, multiple ulcerations, and necrosis. However, co-treated groups

(CTX + MESNA or CTX + *P. dulce*) had minimal bladder damage characterized by reduced leukocyte infiltration, tissue ulceration, and only mild thickening of the lamina propria. Kidney histopathology

of mice treated with CTX showed severe mesangial matrix expansion and hypercellularity in glomeruli and thinning of focal tubular epithelium. In contrast, animals were treated with extract along with CTX prevented the nephrotoxic damage induced by CTX. Liver histopathological analysis of CTX alone treated group showed destructed lobular architecture with centrilobular necrosis surrounded by inflammatory infiltrates and interface hepatitis. In contrast, in animals co-treated with CTX/*P. dulce* group, there was a reduced liver damage, only showing mild sinusoidal dilatation with central vein congestion.

The MCF-7 cells were treated with escalating concentrations of *P. dulce* (1–300 µg/ml). Dose-dependent inhibition in cell proliferation was observed on both 24 hr and 48 hr. IC₅₀ values were determined and it was found to be 164.78 µg/ml and 171.1 µg/ml, respectively (unpublished data).

4 | DISCUSSION

In this study, the chemoprotective activity of *P. dulce* extract against CTX-induced leukopenia was investigated. CTX is an anti-neoplastic immunosuppressive agent used to treat cancer malignancies (Baumann & Preiss, 2001; Fleming, 1997). But it is itself mutagenic, and induces various detrimental effects such as immunotoxicity (Papaldo et al., 2005), urotoxicity (Kiuchi et al., 2009), nephrotoxicity (Amudha, Josephine, Mythili, Sundarapandiyam, & Varalakshmi, 2007), sterility (Qureshi, Pennington, Goldsmith, & Cox, 1972), and hepatotoxicity (Subramaniam, Cader, Mohd, Yen, & Ghafor, 2013). So there is an immediate need for reappraisal of conventional chemotherapeutic strategies while not negating the expected therapeutic effects of the CTX. Combination of immunomodulating agents with chemotherapy may provide new insights into the definition of new and most effective therapeutic strategies for cancer patients.

Here, we examined whether *P. dulce* extract could mitigate the toxicity induced by CTX. CTX is pharmacologically inactive, and undergoes a variety of finely orchestrated complex activation process. CTX is initially biotransformed into 4-hydroxy CTX by microsomal oxidation system in liver, which further gets converted into reactive cytotoxic metabolites such as phosphoramidate mustard and acrolein (Boddy & Yule, 2000; Grochow, 1996). Myelotoxicity and leukopenia are the most common adverse events of CTX treatment. The present investigation revealed that treatment with *P. dulce* extract increased hosts bone marrow cellularity, α -esterase activity, and TLC compared to mice that received CTX only. Altogether, these results suggested that *P. dulce* extract acts possibly through stimulation of hematopoietic system and maturation of monocytes. Moreover, administration of *P. dulce* extract effectively prevented the CTX-induced splenic and thymic weight fall. This indicates the potential role of *P. dulce* extract over CTX-induced immunotoxicity in BALB/c mice.

Nephrotoxicity is another severe toxicity associated with CTX treated patients. Changes in serum levels of urea and creatinine have been found to a fairly reliable indicator of nephrotoxicity. Creatinine

is effectively cleared out from the blood by kidneys through glomerular filtration and proximal tubular secretion. An increment in serum creatinine reflects the disruption of glomerular apparatus. Moreover, renal function can also be analyzed by assessing serum urea level. During protein metabolism, ammonia generated by liver is ultimately transformed into urea. During renal disruption, the rate of serum urea production exceeds the rate of clearance resulting abnormal retention of urea in serum. Here, due to CTX administration, serum levels of urea and creatinine drastically increased, reflecting degree of renal injury. However, co-treatment with *P. dulce* extract significantly reduced serum urea and creatinine, suggesting the potential role of extract from CTX-induced renal damage.

Another serious adverse outcome of CTX treatment is hepatotoxicity. An increment in the levels of serum SGPT, SGOT, and ALP is associated with parenchymal cellular damages and loss of functional integrity of hepatic membrane (Kumar & Kuttan, 2005). Treatment with CTX drastically increased serum SGPT, SGOT, and ALP. The data suggest that hepatic activation of CTX initiates the formation of toxic metabolites which could result in the loss of functional integrity in liver tissues. Co-treatment of *P. dulce* extract along with CTX significantly reduced serum SGPT, SGOT, and ALP indicating its ameliorating role of *P. dulce* extract during CTX-induced liver damage.

Accumulation of urotoxic metabolite of CTX acrolein in urinary bladder for longer period contributes to urinary bladder dysfunction (Cox, 1979; Morais, Belarmon-Filho, Brito, & Ribeiro, 1999). The present investigation revealed that treatment with CTX + MESNA and CTX + *P. dulce* mitigated CTX-induced urinary bladder damage. Studies demonstrated that CTX metabolite accumulation is associated with oxidative stress in the urinary bladder (Ozcan, Korkmaz, Oter, & Coskun, 2005). Molecular oxygen reduction leads to the production of several reactive oxygen species (ROS) that must be immediately scavenged. Under inflammatory conditions, there may be insufficient scavenging of ROS that in turn initiate peroxidative injury resulting in the disruption of the physical state of membrane lipids which may be functionally linked to manifestations of CTX-induced urothelial tissue damage. GSH is the most abundant antioxidant compound within cells and body fluids. Under pro-oxidant conditions, the sulphur moiety of two GSH molecules donates electron and this electron donation converts GSH to GSSH, which can be efficiently converted back to GSH by the action of GSSG reductase. Therefore, a decrease in measured concentrations of GSH is interpreted as evidence of redox imbalance or oxidative stress. Studies have shown that GSH plays a major role in ameliorating acrolein-induced oxidative pathophysiology (MacAllister, Martin-Brisac, Lau, Yang, & O'Brien, 2013; Speen et al., 2015). As expected, in this study, administration of CTX causes a reduction in bladder GSH level while increased LPO level. Treatment with CTX + MESNA and CTX + *P. dulce* reversed these outcomes.

Cytokines are small, non-structural signalling peptides released by cells, including chemokines, interferons, interleukins, and tumor necrotic factors. As the key regulatory molecules of the immune system, global attention is now more than ever turned to understand

the underlying complex effector biological networks. Therefore, studies have been established for the analysis of these essential cellular communication molecules. Treatment with CTX drastically decreased the cytokine levels such as IFN- γ and GM-CSF in normal mice. It should be emphasizing that the lowered levels of these cytokines could be normalized by *P. dulce* extract treatment. These results summarize the enigmatic role of *P. dulce* extract against CTX-induced toxicity, speculate its potential importance for human health.

The immunological, biochemical, and histopathological analysis affirms that methanolic extract of *P. dulce* could effectively protect CTX-induced immunotoxicity, nephrotoxicity, and urothelial toxicity. Further studies are on course to identifying the exact compound in fruit extract of *P. dulce* extract responsible for this protection.

5 | CONCLUSION

In summary, results from this study suggest that *P. dulce* extract could potentially be used to alleviate the toxicity induced by CTX. More comprehensive studies using isolated compounds from this extract will enhance pharmaceutical exploration which will hopefully lead to an improvement in either prevention or treatment strategy of therapy.


ACKNOWLEDGMENTS

The authors acknowledge University Grants Commission (UGC) and Council of Scientific and Industrial Research (CSIR) for providing support in the form of junior research fellowship for the study. The authors are thankful to Dr. Rekha A. Nair, Director, RCC and Dr. S. Kannan, Head, Division of Cancer Research, Regional Cancer Centre (RCC) for providing valuable support required for the study.

CONFLICT OF INTEREST

No conflict of interest.

ORCID

Chandrasekharan Guruvayoorappan  <https://orcid.org/0000-0001-6356-2893>

REFERENCES

- Al-Mamary, M., Al-Habori, M., Al-Aghbaria, A. M., & Baker, M. M. (2002). Investigation to the toxicological effects of *Catha edulis* leaves: A short term study in animals. *Phytotherapy Research*, 16, 127–132. Retrieved from <https://www.ncbi.nlm.nih.gov/pubmed/11933113>
- Amudha, G., Josephine, A., Mythili, Y., Sundarapandian, R., & Varalakshmi, P. (2007). Therapeutic efficacy of dl- α -lipoic acid on cyclosporine A induced renal alterations. *European Journal of Pharmacology*, 571(2–3), 209–214. <https://doi.org/10.1016/j.ejphar.2007.05.047>
- Bancroft, J. D., & Cook, H. C. (1994). Manual of histopathological techniques. *The journal of pathology*, 145, 355–356.
- Baumann, F., & Preiss, R. (2001). Cyclophosphamide and related anticancer drugs. *Journal of Chromatography B: Biomedical Sciences and Applications*, 764, 173–192. [https://doi.org/10.1016/s0378-4347\(01\)00279-1](https://doi.org/10.1016/s0378-4347(01)00279-1)
- Bin-Hafeez, B., Ahmad, I., Haque, R., & Raisuddin, S. (2001). Protective effect of *Cassia occidentalis* L. on cyclophosphamide-induced suppression of humoral immunity in mice. *Journal of Ethnopharmacology*, 75, 13–18. [https://doi.org/10.1016/s0378-8741\(00\)00382-2](https://doi.org/10.1016/s0378-8741(00)00382-2)
- Boddy, A. V., & Yule, S. M. (2000). Metabolism and pharmacokinetics of oxazaphosphorines. *Clinical Pharmacokinetics*, 38, 291–304. Retrieved from <https://www.ncbi.nlm.nih.gov/pubmed/10803453> <https://doi.org/10.2165/00003088-200038040-00001>
- Cox, P. J. (1979). Cyclophosphamide cystitis—Identification of acrolein as the causative agent. *Biochemical Pharmacology*, 28(13), 2045–2049. [https://doi.org/10.1016/0006-2952\(79\)90222-3](https://doi.org/10.1016/0006-2952(79)90222-3)
- Cui, H., Li, T., Wang, L., Su, Y., & Xian, C. J. (2016). *Dioscorea bulbifera* polysaccharide and cyclophosphamide combination enhances anti-cervical cancer effect and attenuates immunosuppression and oxidative stress in mice. *Scientific Reports*, 5, 19185. <https://doi.org/10.1038/srep19185>
- Feng, L., Huang, Q., Huang, Z., Li, H., Qi, X., Wang, Y., ... Lu, L. (2016). Optimized animal model of cyclophosphamide-induced bone marrow suppression. *Basic & Clinical Pharmacology & Toxicology*, 119(5), 428–435. <https://doi.org/10.1111/bcpt.12600>
- Fleming, R. A. (1997). An overview of cyclophosphamide and ifosfamide pharmacology. *Pharmacotherapy*, 17, 1465–1545. Retrieved from <https://www.ncbi.nlm.nih.gov/pubmed/9322882>
- Grochow, L. B. (1996). Covalent DNA-binding drugs. In M. C. Perry (Eds.), *The chemotherapy source book* (pp. 297–299). Baltimore, MD: Williams & Wilkins. Retrieved from <https://www.ncbi.nlm.nih.gov/pubmed/10803453>
- Kiuchi, H., Takao, T., Yamamoto, K., Papaldo, P., Lopez, M., Marolla, P., ... Calabresi, F. (2009). Sesquiterpene lactone parthenolide ameliorates bladder inflammation and bladder overactivity in cyclophosphamide-induced rat cystitis model by inhibiting NF- κ B phosphorylation. *Journal of Urology*, 181, 2339–2348. Retrieved from <https://www.ncbi.nlm.nih.gov/pubmed/16129844>
- Kumar, G., Banu, G. S., Kannan, V., & Pandian, M. R. (2005). Antihepatotoxic effect of beta-carotene on paracetamol induced hepatic damage in rats. *Indian Journal of Experimental Biology*, 43, 351–355. Retrieved from <https://www.ncbi.nlm.nih.gov/pubmed/15875720>
- Kumar, K. B., & Kuttan, R. (2005). Chemoprotective activity of an extract of *Phyllanthus amarus* against cyclophosphamide induced toxicity in mice. *Phytomedicine*, 12, 494–500. <https://doi.org/10.1016/j.phymed.2004.03.009>
- Kumar, M., Govindarajan, J., & Nyola, N. K. (2017). Antihyperglycemic potential of saponin enriched fraction from *Pithecellobium dulce* Benth. Seed Extract. *Pharmacognosy Research*, 9(1), s23–s26. https://doi.org/10.4103/pr.pr_18_17
- López-Angulo, G., Montes-Avila, J., Sánchez-Ximello, L., Díaz-Camacho, S. P., Miranda-Soto, V., López-Valenzuela, J. A., & Delgado-Vargas, F. (2018). Anthocyanins of *Pithecellobium dulce* (Roxb.) Benth. Fruit associated with high antioxidant and α -glucosidase inhibitory activities. *Plant Foods for Human Nutrition*, 73(4), 308–313. <https://doi.org/10.1007/s11130-018-0693-y>
- López-Angulo, G., Verdugo Gaxiola, S. E., Montes-Avila, J., Díaz-Camacho, S. P., Miranda-Soto, V., Salazar Salas, N. Y., & Delgado-Vargas, F. (2019). Bioguided isolation of N-malonyl-(+)-tryptophan from the fruit of *Pithecellobium dulce* (Roxb.) Benth. that showed high activity against *Hymenolepis nana*. *Natural Product Research*, 31, 1–7. <https://doi.org/10.1080/14786419.2019.1590709>

- MacAllister, S. L., Martin-Brisac, N., Lau, V., Yang, K., & O'Brien, P. J. (2013). Acrolein and chloroacetaldehyde: An examination of the cell and cell-free biomarkers of toxicity. *Chemico-Biological Interactions*, 202(1–3), 259–266. <https://doi.org/10.1016/j.cbi.2012.11.017>
- Megala, J., & Geetha, A. (2010). Free radical scavenging and H⁺, K⁺-ATPase inhibition activities of *Pithecellobium dulce*. *Food Chemistry*, 121, 1120–1128. <https://doi.org/10.1016/j.foodchem.2010.01.059>
- Morais, M. M., Belarmono-Filho, J. N., Brito, G. A., & Ribeiro, R. A. (1999). Pharmacological and histopathological study of cyclophosphamide-induced hemorrhagic cystitis-comparison of the effect of dexamethasone and Mesna. *Brazilian Journal of Medical and Biological Research*, 32, 1211–1215. Retrieved from <https://www.ncbi.nlm.nih.gov/pubmed/10510257>
- Ohkawa, H., Ohishi, N., & Yagi, K. (1979). Assay for lipid peroxides in animal tissues by thio-barbituric acid reaction. *Analytical Biochemistry*, 95, 351–358. [https://doi.org/10.1016/0003-2697\(79\)90738-3](https://doi.org/10.1016/0003-2697(79)90738-3)
- Ozcan, A., Korkmaz, A., Oter, S., & Coskun, O. (2005). Contribution of flavonoid antioxidants to the protective effect of mesna in cyclophosphamide-induced cystitis in rats. *Archives of Toxicology*, 8, 461–465. Retrieved from <https://www.ncbi.nlm.nih.gov/pubmed/15800758>
- Papaldo, P., Lopez, M., Marolla, P., Cortesi, E., Antimi, M., Terzoli, E., ... Calabresi, F. (2005). Impact of five prophylactic filgrastim schedules on hematologic toxicity in early breast cancer patients treated with epirubicin and cyclophosphamide. *Journal of Clinical Oncology*, 23(28), 6908–6918. <https://doi.org/10.1200/jco.2005.03.099>
- Pass, G. J., Carrie, D., Boylan, M., Lorimore, S., Wright, E., Houston, B., ... Wolf, C. R. (2005). Role of hepatic cytochrome P450s in the pharmacokinetics and toxicity of cyclophosphamide: Studies with the hepatic cytochrome P450 reductase null mouse. *Cancer Research*, 65, 4211–4217. <https://doi.org/10.1158/0008-5472.can-04-4103>
- Ponmozhi, P., Geetha, M., Saravana Kumar, M., & Suganya devi, P. (2011). Extraction of anthocyanin and analysing its antioxidant properties from *Pithecellobium dulce* fruit pericarp. *Asian Journal of Pharmaceutical and Clinical Research*, 4(1), 41–45. Retrieved from <https://innovareacademics.in/journal/ajpcr/Vol4Suppl1/377.pdf>
- Preethi, S., & Saral, M. (2016). Screening of natural polysaccharides extracted from the fruits of *Pithecellobium dulce* as a pharmaceutical adjuvant. *International Journal of Biological Macromolecules*, 92, 347–356. <https://doi.org/10.1016/j.ijbiomac.2016.07.036>
- Qureshi, M. S. A., Pennington, J. H., Goldsmith, H. J., & Cox, P. J. (1972). Cyclophosphamide therapy and sterility. *Lancet*, 300, 1290–1291. [https://doi.org/10.1016/s0140-6736\(72\)92657-8](https://doi.org/10.1016/s0140-6736(72)92657-8)
- Sahu, N. P., & Mahato, S. B. (1994). Anti-inflammatory triterpene saponins of *Pithecellobium dulce*: Characterization of an echinocystic acid bisdesmoside. *Phytochemistry*, 37(5), 1425–1427. [https://doi.org/10.1016/s0031-9422\(00\)90425-4](https://doi.org/10.1016/s0031-9422(00)90425-4)
- Sakthivel, K. M., & Guruvayoorappan, C. (2015). *Acacia ferruginea* inhibits cyclophosphamide-induced immunosuppression and urotoxicity by modulating cytokines in mice. *Journal of Immunotoxicology*, 12, 154–163. <https://doi.org/10.3109/1547691X.2014.914988>
- Sheeja, K., & Kuttan, G. (2006). Protective effect of *Andrographis paniculata* and andrographolide on cyclophosphamide-induced urothelial toxicity. *Integrative Cancer Therapies*, 5, 244–251. <https://doi.org/10.1177/1534735406291984>
- Singh, K. P., Gupta, R. K., Shau, H., & Ray, P. K. (1993). Effect of ASTA-Z 7575 (INN Maphosphamide) on human lymphokine-activated killer cell induction. *Immunopharmacology and Immunotoxicology*, 15, 525–538. <https://doi.org/10.3109/08923979309019729>
- Speen, A., Jones, C., Patel, R., Shah, H., Nallasamy, P., Brooke, E. A. S., ... Jia, Z. (2015). Mechanisms of CDDO-imidazolide-mediated cytoprotection against acrolein-induced neurocytotoxicity in SH-SY5Y cells and primary human astrocytes. *Toxicology Letters*, 238(1), 32–42. <https://doi.org/10.1016/j.toxlet.2015.07.005>
- Subramaniam, S. R., Cader, R. A., Mohd, R., Yen, K. W., & Ghafor, H. A. (2013). Low-dose cyclophosphamide-induced acute hepatotoxicity. *American Journal of Case Reports*, 14, 345–349. <https://doi.org/10.12659/ajcr.889401>

How to cite this article: Dhanisha SS, Drishya S, Guruvayoorappan C. *Pithecellobium dulce* fruit extract mitigates cyclophosphamide-mediated toxicity by regulating proinflammatory cytokines. *J Food Biochem*. 2019;e13083. <https://doi.org/10.1111/jfbc.13083>

RESEARCH ARTICLE

Molecular Docking Studies of Naringenin and its Protective Efficacy against Methotrexate Induced Oxidative Tissue Injury

Suresh S. Dhanisha¹, Sudarsanan Drishya¹, Karyath P. Gangaraj², Muliya K. Rajesh² and Chandrasekharan Guruvayoorapan^{1,*}

¹Laboratory of Immunopharmacology and Experimental Therapeutics, Division of Cancer Research Regional Cancer Centre, Medical College Campus, Thiruvananthapuram 695011, Kerala, India. (Research centre, University of Kerala); ²Division of Crop Improvement, ICAR-Central Plantation Crops Research Institute, Kasaragod 671124, Kerala, India

Abstract: Background: Although Methotrexate (MTX) possesses a wide clinical spectrum of activity, its toxic side effects on normal cells and drug resistance often hamper its successful outcome. Naringenin (NG) is one of the promising bioactive flavonoids that are extensively found in grapes, citrus fruits, and fruit arils of *Pithecellobium dulce*.

Objective: Only a few experimental *in vivo* studies on the efficacy of NG against chemotherapeutic drugs have been carried out. Aiming to fill this gap, the present study was carried out to characterize and identify its possible therapeutic targets and also to explore its protective efficacy against MTX-induced tissue damage.

Methods: Oxidative stress was induced in mice with MTX (20 mg/kg B.wt), and animals were orally administered with 10 mg/kg B.wt NG for 10 consecutive days. On day 11, all animals were sacrificed, and hematological and serum biochemical parameters were analyzed. The anti-oxidant efficacy of NG against MTX was evaluated by quantifying tissue superoxide dismutase (SOD), glutathione peroxidase (GPx), reduced glutathione (GSH) and catalase along with oxidative stress markers [malondialdehyde (MDA) and nitric oxide (NO)]. Further, the histopathological analysis was performed to confirm the protective efficacy of NG. *In silico* docking studies were also performed to explore anti-oxidant enzyme-based targets.

Results: Our results showed that concurrent administration of NG counteracted oxidative stress induced by MTX, as evidenced by increased expression of anti-oxidant markers, decreased expression of renal and hepatotoxicity serum marker enzymes ($p < 0.05$). A molecular docking study was performed using Auto dock vina to understand the mechanism of ligand binding (S-NG and R-NG) with anti-oxidant enzymes. The binding affinity of S-NG with catalase, GPx, ALP, and SGPT was -10.1, -7.1, -7.1, and -7.3 kcal/mol, respectively, whereas for R-NG was -10.8, -7.1, -7.6, and -7.4 kcal/mol, respectively. Further, histopathological analysis affirmed the protective efficacy of NG against MTX-induced hepatic and renal toxicities.

Conclusion: Treatment with NG significantly reduced MTX-induced pancytopenia, renal, and hepatic toxicity.

Keywords: Methotrexate, naringenin, *in vivo* anti-oxidant activity, toxicity markers, target prediction analysis, molecular docking.

1. INTRODUCTION

Free radicals (oxidants) are generated spontaneously as a byproduct of several cellular metabolic processes [1]. One of the key culprits behind several oxidative stress-related diseases, such as coronary artery disease, hypertension, diabetes, several metabolic syndromes, and cancer [2]. Reactive oxygen species (ROS) in the forms of nitric oxide radical, hydroxyl radical, superoxide radical, and lipid peroxyl radicals are highly reactive, unstable, and have a surplus of unpaired electrons. These ROS can wreak havoc on several important cellular biomolecules such as DNA, proteins, and the cell membrane [3]. Anti-oxidants are free radical scavengers that neutralize the overwhelm radicals by activating a battery of detoxifying proteins and thus contribute to disease prevention. Hence researchers have intensified their quest to identify nontoxic, effective natural product-derived compounds to alleviate free radical mediated-damage.

Current trends of research on flavonoids suggest that they are incredibly important in the alleviation of oxidative stress-associated tissue damages. Due to its broad spectrum of health benefits, it has been considered a vital component in several pharmacological formulations. In this particular study, an attempt has been made to investigate the protective efficacy of flavonoid naringenin (NG) against methotrexate (MTX) induced oxidative tissue damages.

MTX is an antifolate therapeutic agent used against a plethora of malignant and inflammatory disorders. Besides its broad spectrum functions, the detrimental effects on normal healthy cells and drug resistance often hamper its effective disease management [4-11]. To curb these caustic side-effects, several nutraceutical supplements have been tested, among which anti-oxidant supplements have become increasingly popular as an adjuvant in chemotherapy. Such newer therapeutic interventions can enhance the patient's quality of life (QOL). The flavonoid NG is abundantly present in fruit arils of *Pithecellobium dulce* and citrus fruits [12]. It possesses several pharmacological properties, including anti-inflammatory, anti-oxidant, anti-hyperglycemic, and neuroprotective activity [13-16]. However, to the best of our knowledge, no studies have yet reported its protective efficacy against MTX-induced tissue da-

* Address correspondence to this author at the Laboratory of Immunopharmacology and Experimental Therapeutics, Division of Cancer Research, Regional Cancer Centre, Trivandrum-695 011, Kerala, India; Tel: 0471 2522337, +919894337418; E-mail: immunopharmacologyrcc@gmail.com

mages. Hence in the present study, an attempt has been made to evaluate the anti-oxidant efficacy of NG against MTX-induced oxidative stress and associated organ toxicities in Balb/c mice. Further, we have also performed an *insilico* docking study to further confirm the interaction between the bioactive compound NG with key enzymatic anti-oxidants.

2. MATERIALS AND METHODS

2.1. Drugs and Chemicals

Naringenin (NG), silymarin (SLM), and methotrexate (MTX) were purchased from Sigma Aldrich (St. Louis, MO, USA). Riboflavin, sodium nitroprusside (SNP), sulphanilamide, trichloroacetic acid (TCA), and thiobarbituric acid (TBA) were purchased from Hi-Media (Mumbai, India). SDS was obtained from Spectrum Reagents and Chemicals Pvt. Ltd (Kerala, India). Glutathione and 5 dithiobis-2-nitrobenzoic acids (DTNB; Ellman's reagent) were purchased from Molecular Probes Life Technologies (USA). Drabkin's reagent was purchased from Agappe Diagnostics Ltd (Kerala, India). Serum glutamic oxaloacetate transaminase (SGOT), serum glutamate-pyruvate transaminase (SGPT), bilirubin, alkaline phosphatase (ALP), urea and creatinine analyzing kits were purchased from Coral Clinical Systems (Goa, India). All other chemicals used for experimental work were of AR grade.

2.2. Target Prediction Studies

Target prediction study of NG was carried out using the Swiss target prediction tool of the Swiss Institute of Bioinformatics. Canonical smiles were extracted from PubChem and target prediction studies have been carried out.

2.3. Animals

Male Balb/c mice (6-8 weeks old, 22-25 g) were purchased from SreeChitraThirunal Institute for Medical Sciences and Technology (SCTIMST), Thiruvananthapuram. Animals were acclimatized for a period of one month before the study and provided with standard laboratory rodent chow (VRK Nutrition, Maharashtra) and filtered water *ad libidum*. The experimental animals were housed under well-ventilated standard animal housing conditions with a 12-hour light/dark cycle, at the optimal temperature ($25 \pm 2^\circ\text{C}$), and humidity (50%).

2.4. Experimental Design

After acclimatization under laboratory conditions, male Balb/c animals (n=24) were randomly divided into 4 groups (n=6), and each group was caged individually. Group 1 (Control) serves as normal untreated control received 0.1% DMSO as a vehicle. Group 2 (MTX control) received a single dose of MTX (20mg/kg B.wt/p.o) on Day 5. Group 3 (MTX+ SLM) and Group 4 (MTX + NG) received oral administration of SLM (50 mg/kg B.wt.) and NG (10 mg/kg B.Wt), respectively for 10 consecutive days. On the 5th day of the experiment, 1hr after the administration of SLM and NG, Group 3 and 4 were challenged with a single dose of MTX (20mg/kg B.wt/p.o). In all cases, the final material (MTX, SLM, and NG) was resuspended in 0.1% DMSO. On day 11, all animals were euthanized by cervical dislocation. Changes in body weight of all animals were measured initially before the NG administration (Day 0) and then at every 3rd day and continued for 10 days. After euthanization, vital organs of experimental animals were excised and washed with PBS (pH 7.4) and weighed. The final dossiers for organ weight are expressed as relative organ weight (absolute organ weight/body weight of mice x 100). Blood was col-

lected immediately *via* cardiac puncture and used for analyzing hematological parameters such as total leukocyte count (WBC count) and hemoglobin level (Hb). Serum was separated by centrifugation (2000g) and was used for estimating hepatic, and renal toxicity marker enzymes such as SGOT, SGPT, bilirubin, ALP, urea, and creatinine, were measured *via* standard diagnostic kits from Coral Clinical Systems, India. Liver, kidney, and lungs were excised, minced and homogenized (25% (w/v) in ice-cold 0.1 M tris buffer (pH 7.4) using a homogenizer. The resulting homogenate was then used for estimating the level of anti-oxidant enzymes and oxidative stress markers such as catalase, glutathione peroxidase (GPx), total reduced glutathione (GSH) and lipid peroxidation (LPO), nitric oxide (NO), superoxide dismutase (SOD) [17-24]. All data were expressed as mean (\pm standard deviation (SD)).

2.4.1. Docking Study

Molecular docking was performed using web Auto dock Vina [25]. Preparation of appropriate AutoDock Vina input files is prepared using AutoDock software. File preparation by AutoDock involves removing water molecules, adding polar hydrogen atoms, and charging the gasteiger. The energy range has been held as 4, which is set by default. The binding affinity of the ligand with kcal/mol as the unit is observed in a negative score. The results were rendered using an academic edition of the Schrodinger maestro suite [26, 27]. The predicted binding modes with the most favourable Gibbs free energy and the most favorable clustered were analyzed. The structure of the target protein was retrieved using structural information from Protein Data Bank (PDB) and ligand can be selected either by its name or zinc accession number. PDB codes of target proteins are as follows: SGPT-RNG (CHEBI: 50201) /SNG(CHEBI: 17846) (PDB code: 3IHJ), ALP (PDB code: 2GLQ), GPx (PDB code: 2F8A), catalase (PDB code: 1DGF).

2.4.2. Histopathological Examinations

At the end of the experiment, for histopathological analysis, a portion of kidney and liver samples were collected from each experimental group and fixed in 10% formalin solution. The formalin preserved tissue samples were then embedded in paraffin blocks, 4 μm thin sections of tissue samples were prepared in an optical rotary microtome and stained with hematoxylin and eosin (H & E). Further random sections were examined under the microscope (40X magnification).

2.4.3. Statistical Analysis

All the experiments were performed in triplicate. All data are expressed as mean \pm standard deviation (SD). The significant result difference between the groups was determined using one-way ANOVA followed by Dunnett's post hoc test using Instat version 3.0 software (Graphpad, San Diego, CA). p-value less than 0.05 were considered to be statistically significant.

3. RESULTS

3.1. Target Prediction Studies

Insilico screening strategies have been used here to unravel the biological targets of NG. This intervention may help to uncover underlying molecular mechanisms and also to develop new therapeutic strategies for patients with severe incurable diseases. To identify potential targets of NG, the Swiss Target Prediction tool have been used. Several unknown putative drug targets have been identified (Fig. 1).

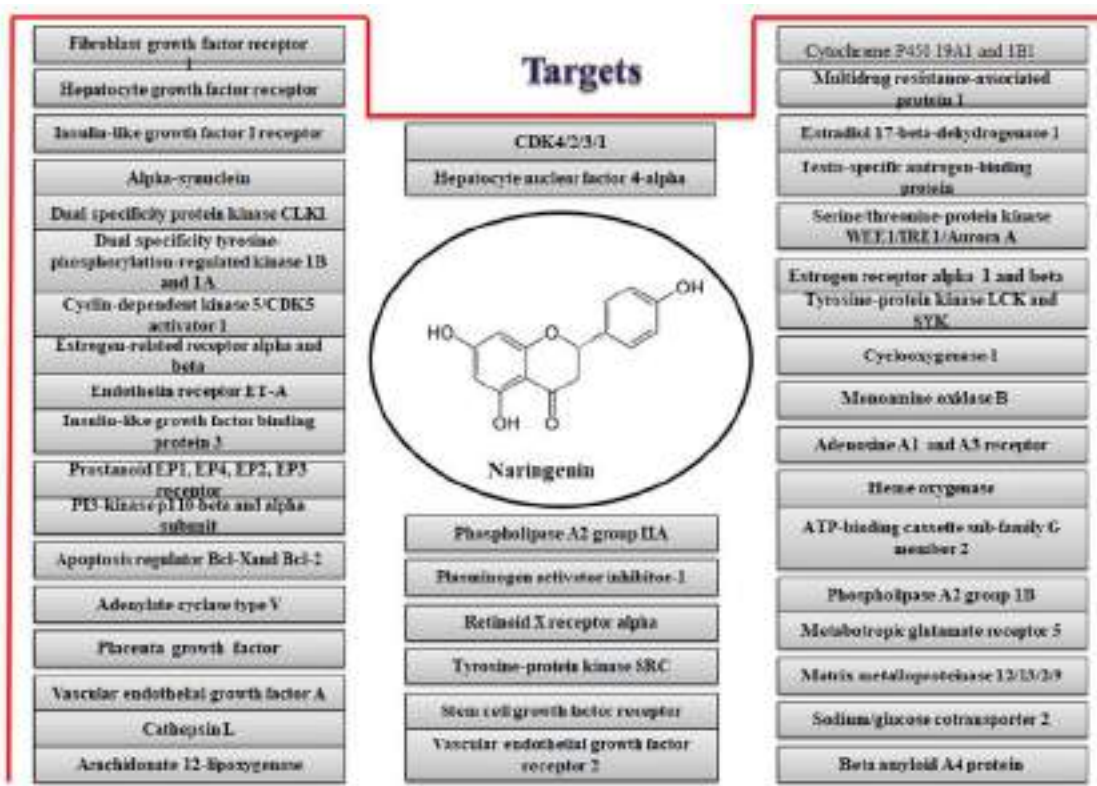


Fig. (1). Schematic representation showing possible targets of naringenin (NG).

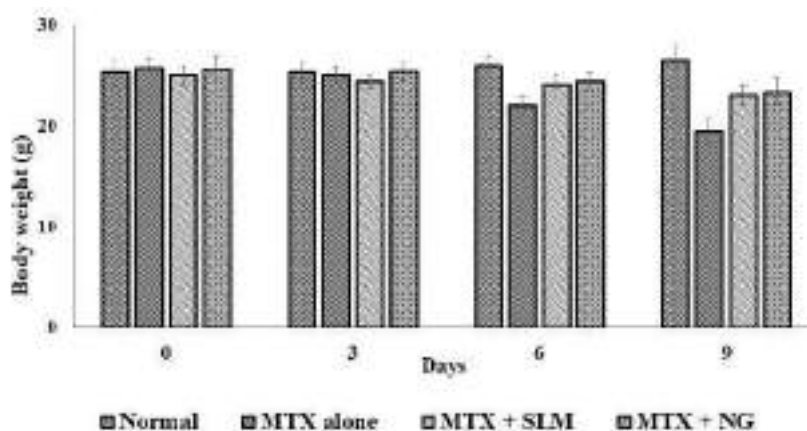


Fig. (2). Assessment of body weight of animals after respective treatments. Body weight of each animal were monitored every 3rd day (starting from day 0 (prior to the first treatment) and statistical analysis were performed. All values shown are mean \pm SD. **p < 0.01, *p < 0.05, for MTX (Methotrexate) alone v/s MTX + SLM (Silymarin) or MTX + NG (naringenin) co-treated.

3.2. Anti-oxidant Studies

3.2.1. Determination of Body Weight, Relative Organ Weight and Hematology Indices

The effect of different treatment regimens on body weight is represented in Fig. (2). Administration of MTX caused a pronounced reduction in body weight on day 9 (19.500 ± 1.29 g) com-

pared to the normal untreated control group (26.500 ± 1.29 g). However, treatment with SLM (23.000 ± 1.00 g) or NG (23.333 ± 1.29 g) with MTX significantly (p < 0.01) attenuated the MTX induced body weight loss.

Table 1 depicts the effects of different treatment regimen on relative organ weight (spleen, thymus, liver, kidney and lungs). MTX administrated group showed a reduced relative organ weight of

Table 1. Effect of NG (Naringenin) on relative organ weight.

Group	Relative organ weight (g/ 100g B.Wt)				
	Spleen	Thymus	Liver	Kidney	Lungs
Normal	0.430 ± 0.03	0.290 ± 0.04	5.770 ± 0.50	1.106 ± 0.06	1.123 ± 0.23
MTX alone	0.270 ± 0.03	0.089 ± 0.03	4.380 ± 0.35	1.270 ± 0.12	0.810 ± 0.05
MTX + SLM	0.390 ± 0.02**	0.170 ± 0.07*	5.628 ± 0.16**	1.310 ± 0.05**	1.110 ± 0.12**
MTX + NG	0.370 ± 0.04**	0.160 ± 0.01*	5.100 ± 0.22**	1.340 ± 0.07**	0.980 ± 0.04**

All values are expressed as mean ± SD. *p <0.05, **p <0.01 compared with MTX alone group

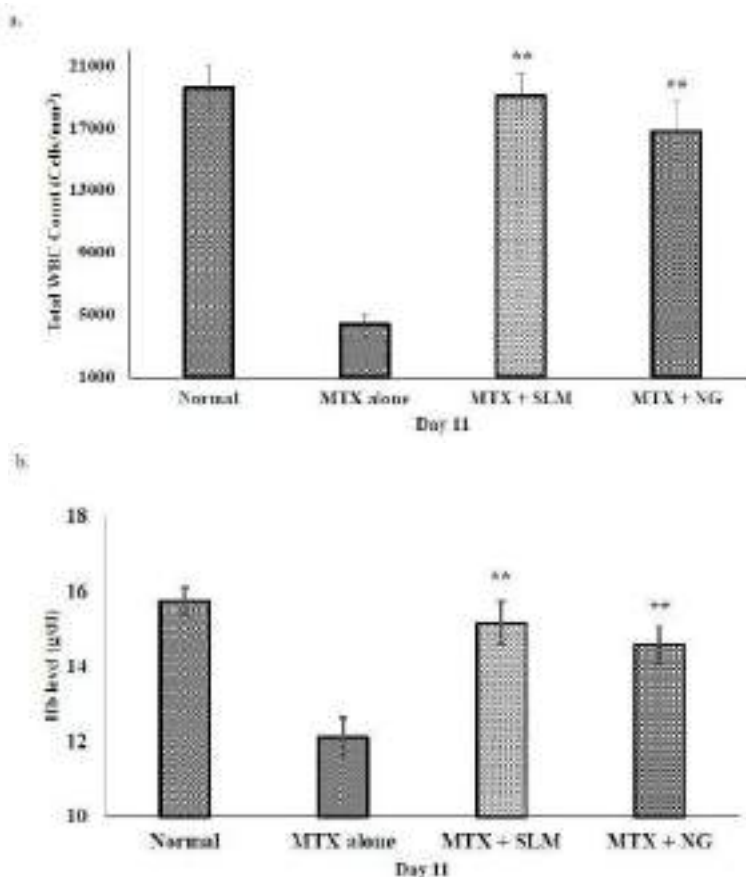


Fig. (3). Effect of different treatment regimens on haematological parameters. Summarizes the effect of NG (naringenin) on a. total leukocyte count (WBC) and b.hemoglobin (Hb) of MTX induced experimental animals. All values shown are mean ± SD. **p <0.01, for MTX (Methotrexate) alone v/s MTX + SLM (Silymarin) or MTX + NG co-treated.

spleen, thymus, liver, kidney and lungs (0.270 ± 0.03 , 0.089 ± 0.03 , 4.380 ± 0.35 , 1.270 ± 0.12 and 0.810 ± 0.05 g/ 100g B.Wt, respectively) compared to normal untreated (0.430 ± 0.03 , 0.290 ± 0.04 , 5.770 ± 0.50 , 1.106 ± 0.06 and 1.123 ± 0.23 g/ 100g B.Wt, respectively). In contrast, combined administration of SLM (0.390 ± 0.02 , 0.170 ± 0.07 , 5.628 ± 0.16 , 1.310 ± 0.05 and 1.110 ± 0.12 g/ 100g B.Wt, respectively) or NG (0.370 ± 0.04 , 0.160 ± 0.01 , 5.100 ± 0.22 , 1.340 ± 0.07 , 0.980 ± 0.04 g/ 100g B.Wt, respectively) with MTX significantly ($p < 0.01$) reversed these changes.

Figure 3a and 3b depict the protective efficacy of NG on haematological parameters. Administration of MTX reduced total leukocyte count (4333.33 ± 755.942 cells/mm³) as well as hemoglobin content (12.09 ± 0.56 g/dL) compared to normal untreated control (19583.33 ± 1527.312 cells/mm³; 15.72 ± 0.37 g/dL, respectively),

whereas treatment with standard drug SLM (19062.50 ± 1314.58 cells/mm³; 15.15 ± 0.57 g/dL, respectively) or NG (16770.50 ± 1881.42 cells/mm³; 14.57 ± 0.52 g/dL, respectively) significantly reinstated the level of total leukocyte count and hemoglobin content to normal.

3.2.2. Effect of different treatment regimens on serum hepatic and renal toxicity marker enzymes

Effect of NG on serum SGOT, SGPT, bilirubin, ALP, urea and creatinine is represented in Table 2 and 3, respectively. MTX administration significantly exacerbated the serum level of hepatic and renal toxicity marker enzymes, such as SGOT, SGPT, bilirubin, ALP, urea and creatinine compared to normal control. The respective values of SGOT, SGPT, bilirubin, urea and creatinine of

Table 2. Effect of NG (Naringenin) on serum SGOT (Serum glutamic oxaloacetic transaminase), SGPT (serum glutamic pyruvic transaminase), bilirubin and ALP (alkaline phosphatase) levels on MTX (Methotrexate) induced experimental animals.

Groups	SGOT (U/L)	SGPT (U/L)	Bilirubin (g/L)	ALP (U/L)
Normal	12.170 ± 3.30	42.400 ± 3.86	0.080 ± 0.03	4.120 ± 0.48
MTX alone	23.420 ± 3.89	84.980 ± 7.44	1.840 ± 0.04	8.560 ± 0.45
MTX + SLM	15.280 ± 3.49 **	45.670 ± 5.78 **	0.170 ± 0.03 **	3.910 ± 0.41 **
MTX + NG	14.780 ± 2.10 **	46.320 ± 3.05 **	1.200 ± 0.05 **	4.170 ± 0.54 **

All values are expressed as mean ± SD. **p < 0.01 compared with MTX alone

Table 3. Effect of NG (Naringenin) on serum urea and creatinine levels on MTX (Methotrexate) induced experimental animals.

Group	Urea (g/L)	Creatinine (g/L)
Normal	1.210 ± 0.05	2.800 ± 0.41
MTX alone	1.840 ± 0.10	3.580 ± 0.31
MTX+ SLM	1.330 ± 0.07 **	3.130 ± 0.08 **
MTX + NG	1.380 ± 0.09 **	3.200 ± 0.12 **

All values are expressed as mean ± SD. **p < 0.01 compared with MTX alone

MTX treated group are as follows, 23.420 ± 3.89 U/L, 84.980 ± 7.44 U/L, 1.840 ± 0.04 g/L, 8.560 ± 0.45 U/L, 1.840 ± 0.10 g/L and 3.580 ± 0.31 g/L, respectively. The respective values of SGOT, SGPT, bilirubin, urea and creatinine of normal control are as follows, 12.170 ± 3.30 U/L, 42.400 ± 3.86 U/L, 0.080 ± 0.03 g/L, 4.120 ± 0.48 U/L, 1.210 ± 0.05 g/L and 2.800 ± 0.41 g/L respectively. However, administration of NG or SLM significantly (p < 0.01) decreased its level compared to MTX group. Their respective values are as follows, NG: 14.780 ± 2.10 U/L, 46.320 ± 3.05 U/L, 1.200 ± 0.05 g/L, 4.170 ± 0.54 U/L, 1.380 ± 0.09 g/L and 3.200 ± 0.12 g/L respectively, SLM: 15.280 ± 3.49 U/L, 45.670 ± 5.78 U/L, 0.170 ± 0.03 g/L, 3.910 ± 0.41 U/L, 1.330 ± 0.07 g/L and 3.130 ± 0.08 g/L respectively.

3.2.3. Analysis of Biochemical Parameters

Figure 4 depicts the level of MDA (lipid peroxidation), NO, SOD, GPx, GSH and catalase on liver, kidney and lungs tissue homogenates. Administration of MTX significantly (p < 0.05) induced oxidative stress in liver, kidney and lungs, as evidenced by the reduced levels of antioxidant enzyme status such as SOD (Fig. 4c) (liver: 0.166 ± 0.02 U/mg protein; kidney: 0.208 ± 0.01 U/mg protein; lungs: 0.129 ± 0.02 U/mg protein), GPx (Fig. 4d) (liver: 2.587 ± 0.19 U/mg protein; kidney: 2.623 ± 0.257 U/mg protein; lungs: 1.285 ± 0.080 U/mg protein), GSH (Fig. 4e) (liver: 69.600 ± 15.88 nmol/mg protein; kidney: 053.916 ± 5.56 nmol/mg protein; lungs: 47.833 ± 7.421 nmol/mg protein) and catalase (Fig. 4f) (liver: 2.178 ± 0.190 μM of H₂O₂ decomposed/min/mg wet tissue; kidney: 0.959 ± 0.190 μM of H₂O₂ decomposed/min/mg wet tissue; lungs: 0.579 ± 0.180 μM of H₂O₂ decomposed/min/mg wet tissue) compared to normal control (SOD: liver: 0.284 ± 0.01 U/mg protein; kidney: 0.253 ± 0.02 U/mg protein; lungs: 0.245 ± 0.03 U/mg protein, GPx: liver: 2.587 ± 0.19 U/mg protein; kidney: 3.967 ± 0.186 U/mg protein; lungs: 2.217 ± 0.087 U/mg protein), GSH: liver: 111.353 ± 10.02 nmol/mg protein; kidney: 87.625 ± 11.15 nmol/mg protein; lungs: 12.030 ± 61.88 nmol/mg protein) and catalase: liver: 4.576 ± 0.32 μM of H₂O₂ decomposed/min/mg wet tissue; kidney: 2.790 ± 0.13 μM of H₂O₂ decomposed/min/mg wet tissue; lungs: 1.788 ± 0.50 μM of H₂O₂ decomposed/min/mg wet tissue. On contrary, the oxidative stress markers such as MDA (LPO) (Fig. 4a) (liver: 9.344 ± 0.838 nmol/mg protein; kidney: 7.211 ± 0.847 nmol/mg protein; lungs: 9.506 ± 0.435 nmol/mg protein) and NO (Fig. 4b) (liver: 172.720 ± 11.999 μM; kidney: 109.828 ± 18.679 μM; lungs: 65.273 ± 14.760 μM) were markedly elevated compared to normal untreated (MDA level: liver: 4.467 ± 1.020 n-

moles/mg protein; kidney: 5.222 ± 0.453 nmol/mg protein; lungs: 5.808 ± 0.874 nmol/mg protein; NO level: liver: 122.207 ± 16.181 μM; kidney: 71.019 ± 16.296 μM; lungs: 53.686 ± 9.424 μM). However, treatment with NG or SLM significantly (p < 0.01) reversed this outcome. The respective values of SOD, GPx, GSH, catalase, MDA (LPO) and NO of liver, kidney and lungs of NG group are as follows. SOD: 0.247 ± 0.018 U/mg protein; kidney: 0.242 ± 0.01 U/mg protein; lungs: 0.231 ± 0.07 U/mg protein, GPx: liver: 4.693 ± 0.21 U/mg protein; kidney: 3.630 ± 0.137 U/mg protein; lungs: 2.066 ± 0.17 U/mg protein, GSH: liver: 90.890 ± 9.93 nmol/mg protein; kidney: 72.120 ± 5.27 nmol/mg protein; lungs: 59.23 ± 5.575 nmol/mg protein, catalase: liver: 3.990 ± 0.28 μM of H₂O₂ decomposed/min/mg wet tissue; kidney: 2.190 ± 0.150 μM of H₂O₂ decomposed/min/mg wet tissue; lungs: 1.240 ± 0.19 μM of H₂O₂ decomposed/min/mg wet tissue, MDA (LPO): liver: 6.121 ± 0.453 nmol/mg protein; kidney: 6.430 ± 0.72 nmol/mg protein; lungs: 1.240 ± 0.19 nmol/mg protein) and NO: liver: 100.600 ± 16.02 μM; kidney: 67.769 ± 15.29 μM; lungs: 72.120 ± 15.45 μM)

3.2.4. Docking Study

Docking of S-NG and R-NG with different anti-oxidant enzymes was performed successfully (Fig. 5). The free energy of binding (ΔG) can be related to the binding affinity ie, lowest value shows greater ligand affinity to the active site of the target protein or the highest binding energy. The highest binding affinity of S-NG with enzyme SGPT was found to be -7.3 kcal/mol. S-NG was found to interact with VAL306, ASN305, ASP304, GLN303, PHE313, ARG312, ARG170, ARG169, and TYR166. S-NG (H 15, O12, and O11 respectively) forms 3 hydrogen bonds with residues ASP 304 (O 2270), PHE313 (H2369), ARG312 (H2356) at a distance of 1.95, 2.24, and 2.04 Å in the vicinity of the catalytic binding pocket of SGPT. The highest binding affinity of S-NG with enzyme ALP was found to be -7.1 kcal/mol. S-NG was found to interact with SEP92, ASP91, VAL89, GLN108, PHE107, HIS432, THR431, GLU430, HIS320, and GLU429. The highest binding affinity of S-NG with enzyme GPx was found to be -7.1 Kcal/mol. S-NG was found to interact with ASN84, LYS86, ASN87, LYS112, ASN77, and GLN82. The highest binding affinity of S-NG with enzyme catalase (O 22) was found to be -10.1 kcal/mol. S-NG was found to interact with SER120, GLU71, ARG68, LYS169, ARG170, PRO172, HIS175, TYR325, PHE326, ASP389, and GLU330. S-NG forms 1 hydrogen bond with residue with SER120 (H 15881) at a distance of 2.35 Å in the vicinity of the

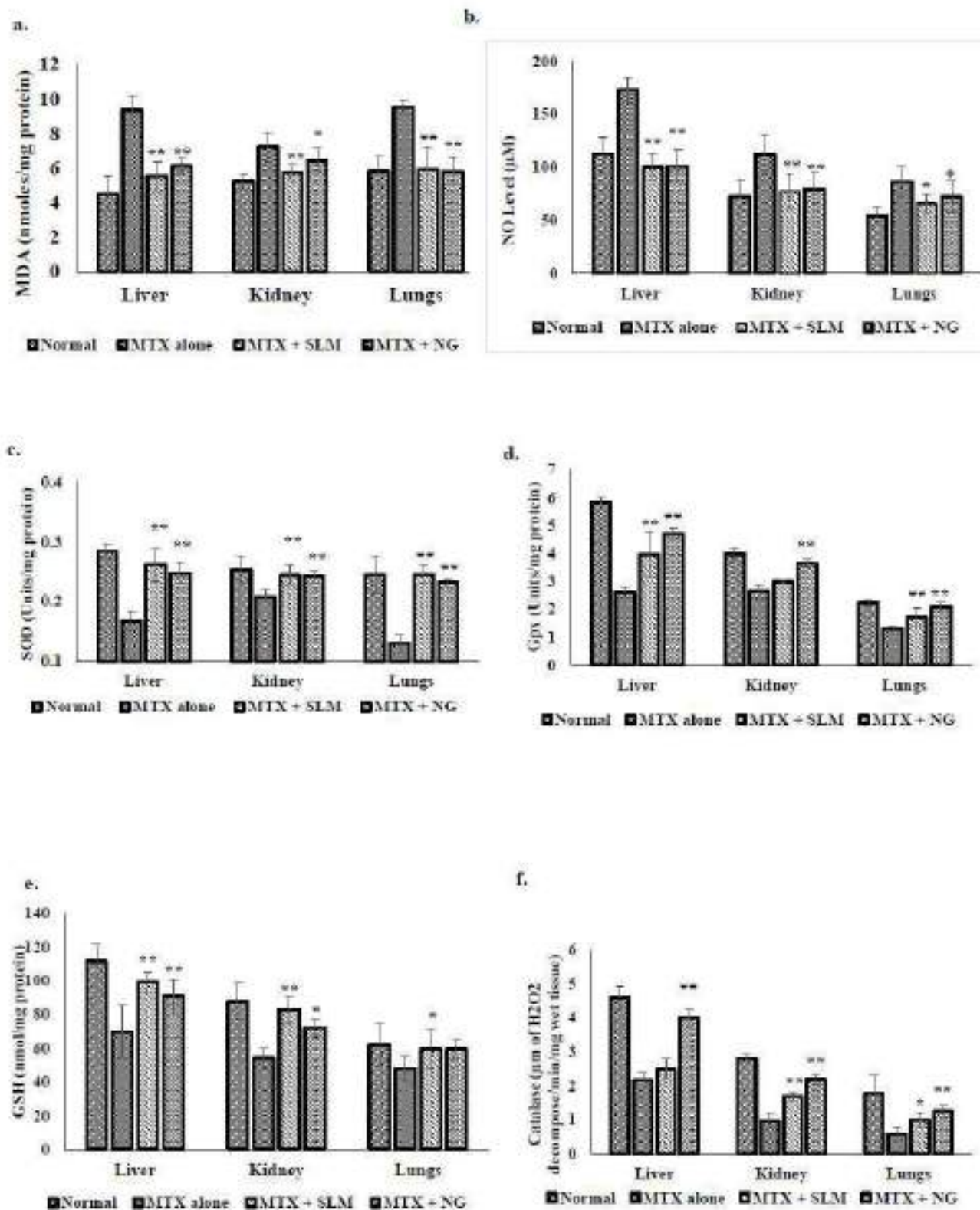


Fig. (4). Liver, kidney and Lungs a. LPO (Lipid peroxidation), b. NO (Nitric oxide), c. SOD (Superoxide dismutase), d. GPx (Glutathione peroxidase), e. GSH (Glutathione) f. Catalase levels after respective treatments. All values shown are mean \pm SD. **p < 0.01, *p < 0.05, for MTX (Methotrexate) alone v/s MTX + SLM (Silymarin) or MTX + NG co-treated.

Table 4.

Target enzyme	Ligand 1: S-Naringenin	Ligand 2: R-Naringenin
Catalase	-10.1 kcal/mol	-10.8 kcal/mol
Glutathione peroxidase (GPx)	-7.1 kcal/mol	-7.1 kcal/mol
Alkaline phosphatase (ALP)	-7.1 kcal/mol	-7.6 kcal/mol
Serum glutamic pyruvic transaminase (SGPT)	-7.3 kcal/mol	-7.4 kcal/mol

Showing the Enzyme -ligand binding affinity (kcal/mol)

Table 5.

Protein	Ligand	H bonds			
		No	Atom in P	Atom in L	Distance (Å)
Catalase	Ligand 1: S-Naringenin	1	Ser120 (H 15881)	O 22	2.35
	Ligand 2: R-Naringenin	1	Arg112(O 1035)	H 15	2.03
Glutathione peroxidase (GPx)	Ligand 1: S-Naringenin	0			
	Ligand 2: R-Naringenin	3	Arg98 (H 840)	O 11	1.97
			Arg98 (H 861)	O 12	2.24
			Gln 82 (H 695)	O 14	2.52
Alkaline phosphatase (ALP)	Ligand 1: S-Naringenin	0			
	Ligand 2: R-Naringenin	1	Gln 108 (H 969)	O 11	2.42
Serum glutamic pyruvic transaminase (SGPT)	Ligand 1: S-Naringenin	3	Asp 304 (O 2270)	H 15	1.95
			Arg 312 (H 2356)	O 11	2.24
			Phe 313 (H 2369)	O 12	2.05
	Ligand 2: R-Naringenin	1	Tyr 343 (H 2663)	O 11	2.63

Showing hydrogen bonding interactions of antioxidant enzymes with ligands S-Naringenin and R-Naringenin

catalytic binding pocket of catalase. The highest binding affinity of R-NG with enzyme SGPT was found to be -7.4 kcal/mol. R-NG was found to interact with TYR343, GLN303, ASP304, VAL306, PHE313, ARG312, ARG170, ARG169, and TYR166. R-NG (O 11) forms 1 hydrogen bond with residue TYR343(H 2663) at a distance of 2.63 Å in the vicinity of the catalytic binding pocket of SGPT. The highest binding affinity of R-NG with enzyme ALP was found to be -7.6 kcal/mol. R-NG (O11) was found to interact with GLN108, PHE107, THR431, HIS432, HIS320, SEP92, HIS917, TYR169, ASN167, and ARG166. R-NG forms 1 hydrogen bond with residue GLN108(H969) at a distance of 2.42 Å in the vicinity of the catalytic binding pocket of ALP. R-NG was found to interact with ASN87, LYS86, ARG98, ASN84, HIS81, GLN82, ASN77, and LEU46. R-NG (H840, H861, and H695) forms 3 hydrogen bonds with residue ARG98 (O11), ARG98(O12), and GLN82(O14) at a distance of 1.97, 2.24, and 2.52 Å in the vicinity of the catalytic binding pocket of GPx. The highest binding affinity of R-NG with enzyme catalase was found to be -10.8 kcal/mol. R-NG was found to interact with ARG112, PHE113, SER114, ALA133, PHE132, GLY131, ASN148, GLY147, VAL146, ARG354, HIS75, VAL74, ARG72, ARG365, HIS362, THR361, and TYR358. R-NG (H 15) forms 1 hydrogen bond with residue with ARG112(O 1035) at a distance of 2.03 Å in the vicinity of the catalytic binding pocket of catalase (Table 4 and 5).

3.2.5. Histopathology

The protective efficacy of NG against MTX-induced pathological changes on kidney and lungs are depicted in Figs. (6 and 7 respectively). The kidney section from the MTX group showed a tubular epithelial loss, mesangial hypercellularity, and inflammatory cell infiltration. Administration of MTX showed severe hepatic damages including altered lobular architecture with focal reactive atypia, bile duct hyperplasia, interface hepatitis, periportal inflammation and cytoplasmic vacuolation. Notably, treatment with NG markedly reduced hepatic and nephrotoxic damage induced by MTX.

4. DISCUSSION

MTX is an antineoplastic agent used as a first-line therapy against autoimmune diseases, cancer, ectopic pregnancy, and medical abortions [28]. However, the therapeutic application of MTX is often restricted due to its severe side effects [29, 30]. The mechanism underlying MTX-induced oxidative tissue injury is not well understood, however, its toxic effects are known to be mediated by increased production of free radicals. Excessive generation of ROS debilitates anti-oxidant defense capacity and leads to excessive oxidative stress. Cells are protected against oxidative stress-associated tissue damages by an interacting network of both enzymatic (SOD, GPx, and catalase) and non-enzymatic anti-oxidants (vitamin E, melatonin, uric acid, GSH, and ascorbic acid) [31]. Studies have shown that the administration of MTX significantly reduces the efficiency of anti-oxidant defense mechanisms in tissues such as the liver, lungs, and kidney, which was demonstrated as a reduction in cellular anti-oxidant enzymes such as SOD, GSH, GPx, and catalase. On the other hand, it induces the level of oxidative stress markers such as MDA and NO. Anti-oxidants are molecules that are stable enough to donate an electron to free radical and neutralize it, thus delay or inhibit oxidative stress-mediated adverse effects induced by drugs. Thus, it is worthwhile to design a novel combinational therapeutic strategy with anti-oxidant agents that could reduce MTX induced toxicity and enhance its efficacy.

Plant-derived flavonoids have been reported to reduce ROS in cells. NG is one of the active flavonoids in citrus fruits and *Pithecellobium dulce* has been reported to exhibit potent anti-oxidant and health-promoting properties. In this present study, the beneficial effects of NG over MTX have been analyzed. As expected, in accordance with the reports of other findings, reductions in anti-oxidant enzymes in tissues (SOD, catalase, GSH, and GPx) were observed following MTX administration. The combined therapy of MTX with NG showed an increased level of tissue anti-oxidant status markers and reduced oxidative stress markers (LPO (MDA) and NO) in the liver, kidney, and lungs, which evinced its explicit

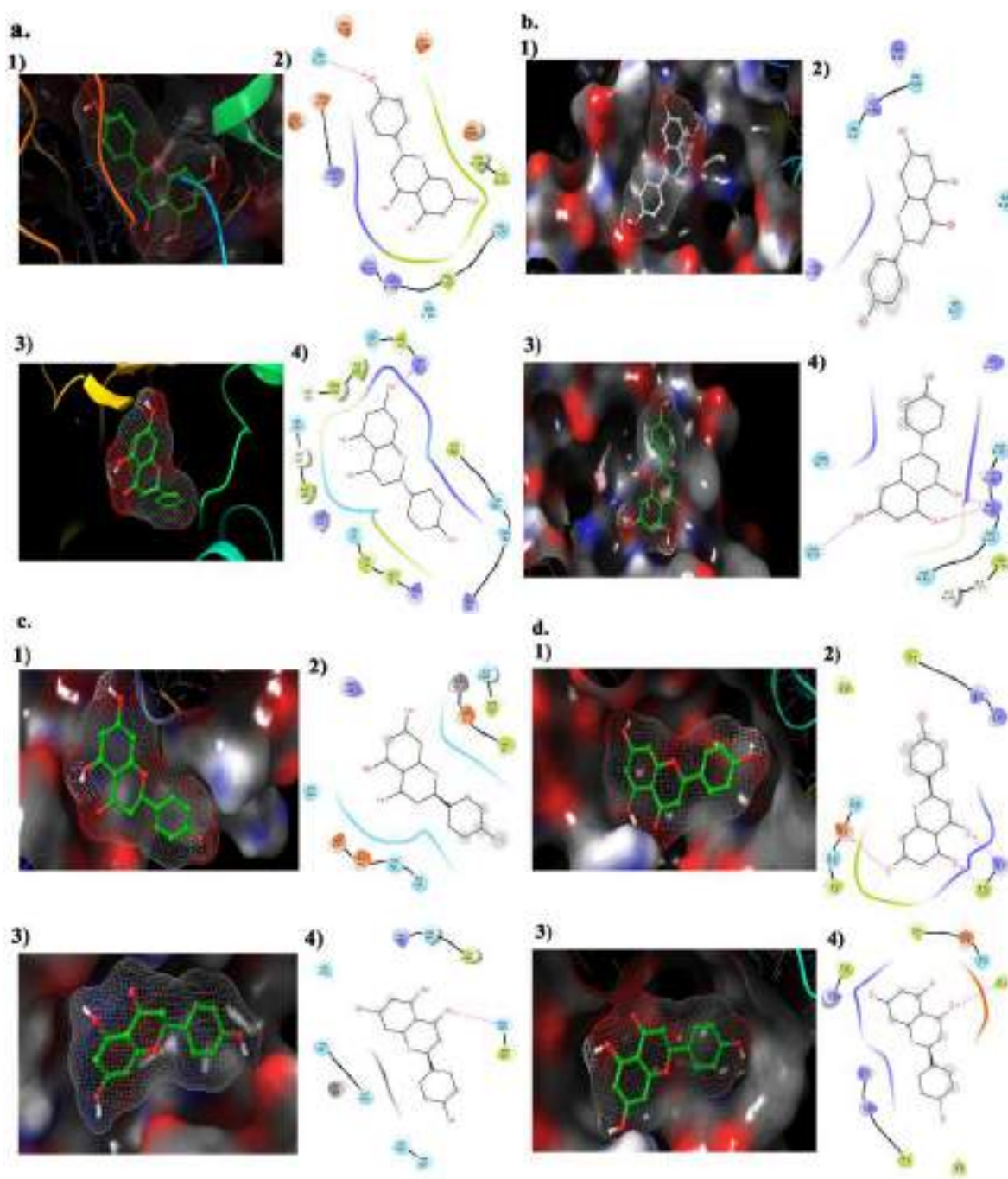


Fig. (5). Schematic representation showing interaction of naringenin (*S*-NG and *R*-NG) with a.1: Interaction complex formed between catalase protein and ligand *S*-NG 2: Interaction diagram of catalase protein and ligand *S*-NG. The violet arrow mark denotes hydrogen bond.3: Interaction complex formed between catalase protein and ligand *R*-NG 4: Interaction diagram of catalase protein and ligand *R*-NG. The violet arrow mark denotes hydrogen bond. b. 1. Interaction complex formed between GPx(Glutathione peroxidase) protein and ligand *S*-NG 2: Interaction diagram of GPx protein and ligand *S*-NG 3: Interaction complex formed between GPx protein and *R*-NG 4: Interaction diagram of GPx protein and ligand *R*-NG. The violet arrow mark denotes hydrogen bond. c.1. Interaction complex formed between ALP (Alkaline phosphatase) protein and ligand *S*-NG 2: Interaction diagram of ALP protein and ligand *S*-NG 3: Interaction complex formed between ALP protein and ligand *R*-NG 4: Interaction diagram of ALP protein and ligand *R*-NG. The violet arrow mark denotes hydrogen bond. d.1. Interaction complex formed between SGPT (Serum glutamic pyruvic transaminase) protein and ligand *S*-NG 2: Interaction diagram of SGPT protein and ligand *S*-NG. The blue arrow mark denotes hydrogen bond. 3. Interaction complex formed between SGPT protein and ligand *R*-NG 4: Interaction complex formed between SGPT protein and ligand *S*-NG. The blue arrow mark denotes hydrogen bond.

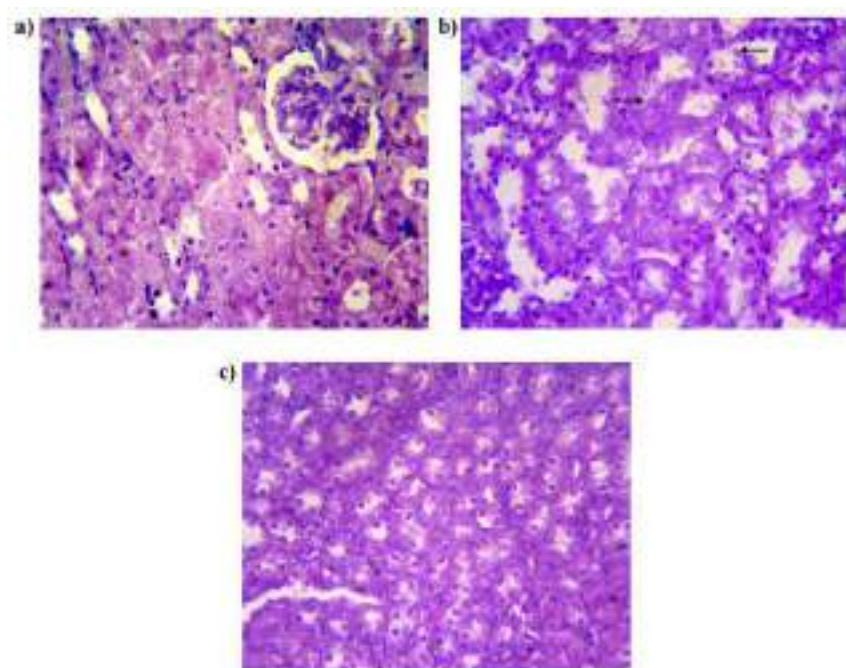


Fig. (6). Protective effect of NG (naringenin) on kidney histology during MTX (Methotrexate) induced toxicity. Photomicrograph of a mouse kidney after respective treatments is represented here. a. Section from normal mice: Showed normal histology b. MTX alone group: the glomeruli showed mild mesangial hypercellularity, matrix expansion and focal necrosis. MTX + NG: the glomeruli showed mild mesangial expansion. (Magnification-40X). Arrow marks represent tubular epithelial loss and cytoplasmic vacuolation and inflammatory cell infiltration.

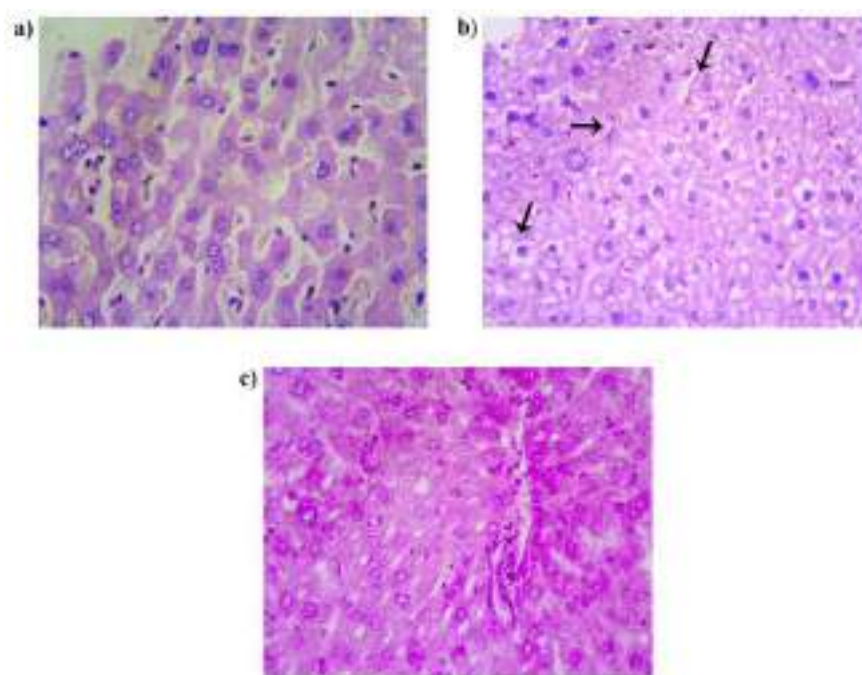


Fig. (7). Protective effect of NG (naringenin) on liver histology during MTX (Methotrexate) induced toxicity. Photomicrograph of a mouse kidney after respective treatments is represented here. a. Section from normal mice: showed normal histology b. MTX alone group: Section showed altered lobular architecture with interface hepatitis, inflammatory infiltration c. MTX + NG: Showed normal lobular architecture with interface hepatitis. Individual hepatocytes showed no significant pathology. (Magnification-40X). Arrow marks represent periportal inflammation and cytoplasmic vacuolation.

role against MTX associated oxidative damages. For further validation computational docking approach has been used [32]. Molecular docking is a computational approach used to predict the non-covalent binding of small drug-like molecules to target proteins [33, 34]. Here docking analysis of different isomers of NG with anti-oxidant enzymes was performed using Autodoc vina. Further, optimized structures of *S*-NG, *R*-NG, and different anti-oxidant enzymes such as catalase, SGPT, AST, and GPx have been used for predicting possible bound conformations and binding affinity. Our results showed a strong binding affinity of NG with anti-oxidant enzymes, which was further confirmed by its efficacy to ameliorate oxidative stress induced by MTX. Corroborating these findings, it can be speculated that NG imparts their protective effect possibly *via* interacting with anti-oxidant enzymes.

Another most frequent hematological disorder associated with MTX induced toxicity is pancytopenia [35]. Co-administration of NG significantly debilitated MTX induced leucopenia and myelotoxicity. Moreover, this combinational approach also showed a remarkable effect against MTX induced thymic and splenic relative organ weight fall. It manifested the key protective role of NG over MTX induced pancytopenia.

Another most common dreadful complication associated with chronic MTX treatment is hepatotoxicity [36, 37]. The rise in serum levels of hepatic toxicity marker enzymes such as SGPT, ALP, bilirubin, and SGOT could be probably due to alterations in the structural integrity of the hepatic biological membrane induced by MTX. Another adverse consequence of chronic MTX therapy is nephrotoxicity. Elevation in serum urea and creatinine could be possibly due to tubular destruction induced by MTX and its metabolites. In agreement with the known data, our results also showed elevated levels of hepatic-nephrotoxicity marker enzymes. However, co-administration of NG with MTX significantly reduced MTX induced serum hepatic-nephrotoxicity marker enzymes, indicating its invincible hepatic and nephron protective property over MTX induced hepatotoxicity. Further, histopathology analysis confirmed the hepatic-nephroprotective efficacy of NG over MTX.

NG contains a functional active group, a 2,3-double bond linked to the 4-oxo group, and this critical group scavenges the free radicals, which is an underlying mechanism responsible for their bioactivities [38, 39]. Studies have shown that NG at a lethal dose (LD)₅₀ of 5000 mg/kg B.wt is found to be relatively safe [40]. NG has been reported to have protective effect against non-alcoholic liver disease by down-regulating NLRP3/NF- κ B pathway in mice models [41]. Studies were reported to possess anti-inflammatory [42], anti-oxidant [43], anticancer, cardioprotective [44], anti-microbial [45] and anti-viral effect [46]. NG reduced body weight and insulin resistance, and increased metabolic rate by peroxisome proliferator activated receptor-alpha (PPAR- α) and peroxisome proliferator activated receptor-beta (PPAR- β) activation. Supplementation of NG on experimental autoimmune encephalomyelitis mice attenuates chemokine mediated migration of dendritic cells and pathogenic infiltration of T cells in central nervous system (CNS) [47]. Another study have showed the protective efficacy of NG on cell line system and mice models against sodium iodate induced oxidative damage *via* upregulation of sirtuin 1 (SIRT1) [48]. Interaction between ligand and enzymes are often stereospecific. The anti-oxidant efficacy of NG is further confirmed by molecular docking studies. *In silico* target prediction approaches are gaining the utmost importance in recent years. The use of complementary experimental and sophisticated *in silico* bioinformatics approaches has given a tremendous opportunity to evaluate the unexplored target identification of a potential drug. Docking poses of enantiomers of NG (*S* and *R* form) with different anti-oxidant enzymes such as SGPT, ALP, GPx, and catalase were analyzed. The best binding affinity of

S-NG with SGPT, ALP, GPx, and catalase is found to be -7.3, -7.1, -7.1, and -10.1 kcal/mol, respectively and that of *R*-NG was found to be -7.4, -7.6, -7.1 and -10.8 kcal/mol respectively. *S*-NG forms 3 hydrogen bonds and *R*-NG forms 1 hydrogen bond at a distance of 1.95, 2.24, 2.04, and 2.63 Å, respectively, in the vicinity of the catalytic binding pocket of SGPT. *R*-NG forms 1 hydrogen bond at a distance of 2.42 Å in the catalytic binding pocket of ALP. *R*-NG forms 3 hydrogen bonds with catalytic binding residue of the enzyme GPx at a distance of 1.97, 2.24, and 2.52 Å. *S*-NG and *R*-NG form 1 hydrogen bond at a distance of 2.35 and 2.03 Å respectively in the vicinity of the catalytic binding pocket of catalase. Based on the obtained finding, NG is a potent anti-oxidant, has a strong binding affinity with different key anti-oxidant proteins in the biological system.

CONCLUSION

In this particular study, we confirmed the protective efficacy of NG against oxidative damages induced by MTX. Herein we also explored the putative biological targets of NG using Swiss-Prot. The knowledge of these targets may uncover its mechanisms of action and beyond. Administration of NG significantly ameliorated MTX-induced toxicity *via* regulating oxidative defense system, thus preventing lipid peroxidation. However, the efficient parallelization of ensemble molecular docking analysis along with *in vivo* study provides lucrative comprehensive data suggesting the therapeutic potential of NG.

ETHICS APPROVAL AND CONSENT TO PARTICIPATE

All animal experimental procedures were carried out after obtaining approval from Institutional Animals Ethics Committee (I-AEC), Regional Cancer Centre (RCC), Thiruvananthapuram, Kerala (IAEC/RCC NO. 6/18). No human samples were used for studies.

HUMAN AND ANIMAL RIGHTS

No humans were used in this study. All animals' research procedure were in accordance with the standards set forth in the 8th Edition of Guide for the Care and Use of Laboratory Animals (<http://grants.nih.gov/grants/olaw/Guide-for-the-care-and-use-of-laboratory-animals.pdf>).

CONSENT FOR PUBLICATION

Not applicable.

AVAILABILITY OF DATA AND MATERIALS

Not applicable.

FUNDING

This study was funded by the Council of Scientific and Industrial Research University Grants Commission [20/12/2015 (ii) EU-V] and [09/553(0022)/2016-EMR-1].

CONFLICT OF INTEREST

The authors declare no conflicts of interest, financial or otherwise.

ACKNOWLEDGEMENTS

Dhanisha S S and Drishya Sudarsanan acknowledges Council of Scientific and Industrial Research University Grants Commission [20/12/2015 (ii) EU-V] and [09/553(0022)/2016-EMR-1] respectively for providing support in the form of senior research fel-

lowship for the study. The authors are thankful to Dr. Rekha. A. Nair, Director, Regional Cancer Centre (RCC) and Dr. S. Kannan, Head, Division of Cancer Research, RCC for providing valuable support required for the study.

REFERENCES

- Cheeseman, K.H.; Slater, T.F. An introduction to free radical biochemistry. *Br. Med. Bull.*, **1993**, *49*(3), 481-493. <http://dx.doi.org/10.1093/oxfordjournals.bmb.a072625> PMID: 8221017
- Bagchi, K.; Puri, S. Free radicals and antioxidants in health and disease. *East. Mediterr.*, **1998**, *14*, 350-360.
- Dröge, W. Free radicals in the physiological control of cell function. *Physiol. Rev.*, **2002**, *82*(1), 47-95. <http://dx.doi.org/10.1152/physrev.00018.2001> PMID: 11773609
- Oren, R.; Moshkowitz, M.; Odes, S.; Becker, S.; Keter, D.; Pomeranz, I.; Shirin, H.; Reisfeld, I.; Broide, E.; Lavy, A.; Fich, A.; Eliakim, R.; Patz, J.; Villa, Y.; Arber, N.; Gilat, T. Methotrexate in chronic active Crohn's disease: a double-blind, randomized, Israeli multicenter trial. *Am. J. Gastroenterol.*, **1997**, *92*(12), 2203-2209. PMID: 9399753
- Kitumara, M.; Kitumara, S.; Fujioka, M.; Kamijo, R.; Shinya, S.; Sawayama, Y.; Uramatsu, T.; Obata, Y.; Mochizuki, Y.; Nishikido, M.; Sakai, H.; Miyazaki, Y.; Mukae, H.; Nishino, T. Methotrexate-induced acute kidney injury in patients with hematological malignancies: three case reports with literature review. *Ren. Replace. Ther.*, **2018**, *4*, 39. <http://dx.doi.org/10.1186/s41100-018-0180-9>
- Widemann, B.C.; Adamson, P.C. Understanding and managing methotrexate nephrotoxicity. *Oncologist*, **2006**, *11*(6), 694-703. <http://dx.doi.org/10.1634/theoncologist.11-6-694> PMID: 16794248
- Conway, R.; Carey, J.J. Risk of liver disease in methotrexate treated patients. *World J. Hepatol.*, **2017**, *9*(26), 1092-1100. <http://dx.doi.org/10.4254/wjh.v9.i26.1092> PMID: 28989565
- Bath, R.K.; Brar, N.K.; Forouhar, F.A.; Wu, G.Y. A review of methotrexate-associated hepatotoxicity. *J. Dig. Dis.*, **2014**, *15*(10), 517-524. <http://dx.doi.org/10.1111/1751-2980.12184> PMID: 25139707
- Jakubovic, B.D.; Donovan, A.; Webster, P.M.; Shear, N.H. Methotrexate-induced pulmonary toxicity. *Can. Respir. J.*, **2013**, *20*(3), 153-155. <http://dx.doi.org/10.1155/2013/527912> PMID: 23762881
- Lateef, O.; Shakoob, N.; Balk, R.A. Methotrexate pulmonary toxicity. *Expert Opin. Drug Saf.*, **2005**, *4*(4), 723-730. <http://dx.doi.org/10.1517/14740338.4.4.723> PMID: 16011450
- Gonzalez-Ibarra, F.; Eivaz-Mohammadi, S.; Surapaneni, S.; Alsaadi, H.; Syed, A.K.; Badin, S.; Marian, V.; Elamir, M. Methotrexate induced pancytopenia. *Case Rep. Rheumatol.*, **2014**, *2014*, 679580. <http://dx.doi.org/10.1155/2014/679580> PMID: 25006519
- Dhanisha, S.S.; Drishya, S.; Guruvayoorappan, C. *Pithecellobium dulce* fruit extract mitigates cyclophosphamide-mediated toxicity by regulating proinflammatory cytokines. *J. Food Biochem.*, **2020**, *44*(1), e13083. <http://dx.doi.org/10.1111/jfbc.13083> PMID: 31633209
- Xue, N.; Wu, X.; Wu, L.; Li, L.; Wang, F. Antinociceptive and anti-inflammatory effect of Naringenin in different nociceptive and inflammatory mice models. *Life Sci.*, **2019**, *217*, 148-154. <http://dx.doi.org/10.1016/j.lfs.2018.11.013> PMID: 30414428
- Cavia-Saiz, M.; Busto, M.D.; Pilar-Izquierdo, M.C.; Ortega, N.; Perez-Mateos, M.; Muñoz, P. Antioxidant properties, radical scavenging activity and biomolecule protection capacity of flavonoid naringenin and its glycoside naringin: a comparative study. *J. Sci. Food Agric.*, **2010**, *90*(7), 1238-1244. <http://dx.doi.org/10.1002/jsfa.3959> PMID: 20394007
- Annadurai, T.; Muralidharan, A.R.; Joseph, T.; Hsu, M.J.; Thomas, P.A.; Geraldine, P. Antihyperglycemic and antioxidant effects of a flavanone, naringenin, in streptozotocin-nicotinamide-induced experimental diabetic rats. *J. Physiol. Biochem.*, **2012**, *68*(3), 307-318. <http://dx.doi.org/10.1007/s13105-011-0142-y> PMID: 22234849
- Raza, S.S.; Khan, M.M.; Ahmad, A.; Ashfaq, M.; Islam, F.; Wagner, A.P.; Safhi, M.M.; Islam, F. Neuroprotective effect of naringenin is mediated through suppression of NF- κ B signaling pathway in experimental stroke. *Neuroscience*, **2013**, *230*, 157-171. <http://dx.doi.org/10.1016/j.neuroscience.2012.10.041> PMID: 23103795
- Chance, B.; Maehly, A.C. Assay of catalases and peroxidases. *Methods Enzymol.*, **1955**, *136*, 764-775. [http://dx.doi.org/10.1016/S0076-6879\(55\)02300-8](http://dx.doi.org/10.1016/S0076-6879(55)02300-8)
- Flohé, L.; Günzler, W.A. Assays of glutathione peroxidase. *Methods Enzymol.*, **1984**, *105*, 114-121. [http://dx.doi.org/10.1016/S0076-6879\(84\)05015-1](http://dx.doi.org/10.1016/S0076-6879(84)05015-1) PMID: 6727659
- Moron, M.S.; Depierre, J.W.; Mannervik, B. Levels of glutathione, glutathione reductase and glutathione-S-transferase activities in rat lung and liver. *Biochem. Biophys. Acta*, **1979**, *582*(1), 67-78. [http://dx.doi.org/10.1016/0304-4165\(79\)90289-7](http://dx.doi.org/10.1016/0304-4165(79)90289-7)
- Bishayee, S.; Balasubramanian, A.S. Lipid peroxide formation in rat brain. *J. Neurochem.*, **1971**, *18*(6), 909-920. <http://dx.doi.org/10.1111/j.1471-4159.1971.tb12020.x> PMID: 4398119
- Ohkawa, H.; Ohishi, N.; Yagi, K. Assay for lipid peroxides in animal tissues by thiobarbituric acid reaction. *Anal. Biochem.*, **1979**, *95*(2), 351-358. [http://dx.doi.org/10.1016/0003-2697\(79\)90738-3](http://dx.doi.org/10.1016/0003-2697(79)90738-3) PMID: 36810
- Green, L.C.; Wagner, D.A.; Glogowski, J.; Skipper, P.L.; Wishnok, J.S.; Tannenbaum, S.R. Analysis of nitrate, nitrite, and [15N]nitrate in biological fluids. *Anal. Biochem.*, **1982**, *126*(1), 131-138. [http://dx.doi.org/10.1016/0003-2697\(82\)90118-X](http://dx.doi.org/10.1016/0003-2697(82)90118-X) PMID: 7181105
- Marcocci, L.; Maguire, J.J.; Droy-Lefaix, M.T.; Packer, L. The nitric oxide-scavenging properties of Ginkgo biloba extract Egb 761. *Biochem. Biophys. Res. Commun.*, **1994**, *201*(2), 748-755. <http://dx.doi.org/10.1006/bbrc.1994.1764> PMID: 8003011
- McCord, J.M.; Fridovich, I. Superoxide dismutase. An enzymic function for erythrocyte (hemocuprein). *J. Biol. Chem.*, **1969**, *244*(22), 6049-6055. [http://dx.doi.org/10.1016/S0021-9258\(18\)63504-5](http://dx.doi.org/10.1016/S0021-9258(18)63504-5) PMID: 5389100
- Trott, O.; Olson, A.J. AutoDock Vina: improving the speed and accuracy of docking with a new scoring function, efficient optimization, and multi-threading. *J. Comput. Chem.*, **2010**, *31*(2), 455-461. <http://dx.doi.org/10.1002/jcc.21334> PMID: 19499576
- David, T.I.; Adelakun, N.S.; Omotuyi, O.I.; Metibemu, D.S.; Ekun, O.E.; Eniafe, G.O.; Inyang, O.K.; Adewumi, B.; Enejoh, O.A.; Owolabi, R.T.; Oribamise, E.I. Molecular docking analysis of phyto-constituents from Cannabis sativa with pDHFHFR. *Bioinformation*, **2018**, *14*(9), 574-579. <http://dx.doi.org/10.6026/97320630014574> PMID: 31223216
- Lewars, E. *Computational chemistry: introduction to the theory and applications of molecular and quantum mechanics*, 2nd ed; Springer publications: Netherlands, **2011**. <http://dx.doi.org/10.1007/978-90-481-3862-3>
- Khan, Z.A.; Tripathi, R.; Mishra, B. Methotrexate: a detailed review on drug delivery and clinical aspects. *Expert Opin. Drug Del.*, **2012**, *9*(2), 151-169. <http://dx.doi.org/10.1517/17425247.2012.642362>
- Hersh, E.M.; Wong, V.G.; Henderson, E.S.; Freireich, E.J. Hepatotoxic effects of methotrexate. *Cancer*, **1966**, *19*(4), 600-606. [http://dx.doi.org/10.1002/1097-0142\(196604\)19:4<600::AID-CNCR2820190420>3.0.CO;2-3](http://dx.doi.org/10.1002/1097-0142(196604)19:4<600::AID-CNCR2820190420>3.0.CO;2-3) PMID: 5933584
- Hall, P.D.; Jenner, M.A.; Ahern, M.J. Hepatotoxicity in a rat model caused by orally administered methotrexate. *Hepatology*, **1991**, *14*(5), 906-910. <http://dx.doi.org/10.1002/hep.1840140525> PMID: 1937394
- Miyazono, Y.; Gao, F.; Horie, T. Oxidative stress contributes to methotrexate-induced small intestinal toxicity in rats. *Scand. J. Gastroenterol.*, **2004**, *39*(11), 1119-1127. <http://dx.doi.org/10.1080/00365520410003605> PMID: 15545171
- Lim, A.Y.N.; Gaffney, K.; Scott, D.G. Methotrexate-induced pancytopenia: serious and under-reported? Our experience of 25 cases in 5 years. *Rheumatology (Oxford)*, **2005**, *44*(8), 1051-1055. <http://dx.doi.org/10.1093/rheumatology/keh685> PMID: 15901903
- Dong, D.; Xu, Z.; Zhong, W.; Peng, S. Parallelization of molecular docking: a review. *Curr. Top. Med. Chem.*, **2018**, *18*(12), 1015-1028. <http://dx.doi.org/10.2174/1568026618666180821145215> PMID: 30129415
- Jakhar, R.; Dangi, M.; Khichi, A.; Chhillar, A.K. Relevance of molecular docking in drug designing. *Curr. Bioinform.*, **2020**, *15*(4), 270-278. <http://dx.doi.org/10.2174/1574893615666191219094216>
- Saikia, S.; Bordoloi, M. Molecular docking: challenges, advances and its use in drug discovery perspective. *Curr. Drug Targets*, **2019**, *20*(5), 501-521. <http://dx.doi.org/10.2174/1389450119666181022153016> PMID: 30360733
- Tousson, E.; Atteya, E.; El-Attrash, E.; Jeweely, O.I. Abrogation by Ginkgo Biloba leaf extract on hepatic and renal toxicity induced by methotrexate in rats. *J. Cancer Res. Treat.*, **2014**, *2*(3), 44-51. <http://dx.doi.org/10.12691/jcrt-2-3-1>
- Abdel-Daim, M.M.; Khalifa, H.A.; Abushouk, A.I.; Dkhil, M.A.; Al-Quraishy, S.A. *Diosmin Attenuates Methotrexate-Induced Hepatic, Renal, and Cardiac Injury: A Biochemical and Histopathological Study in Mice*; Oxida. Med. Cell Longev. **2017**, pp. 1-10.
- Kumar, S.; Pandey, A.K. Chemistry and biological activities of flavonoids: an overview. *ScientificWorldJournal*, **2013**, *2013*, 162750. <http://dx.doi.org/10.1155/2013/162750> PMID: 24470791
- Ji, P.; Yu, T.; Liu, Y.; Jiang, J.; Xu, J.; Zhao, Y.; Hao, Y.; Qiu, Y.; Zhao, W.; Wu, C. Naringenin-loaded solid lipid nanoparticles: preparation, controlled delivery, cellular uptake, and pulmonary pharmacokinetics. *Drug Des. Devel. Ther.*, **2016**, *10*, 911-925. PMID: 27041995
- Ortiz-Andrade, R.R.; Sánchez-Salgado, J.C.; Navarrete-Vázquez, G.; Webster, S.P.; Binnie, M.; García-Jiménez, S.; León-Rivera, I.; Cigarroa-Vázquez, P.; Villalobos-Molina, R.; Estrada-Soto, S. Antidiabetic and toxicological evaluations of naringenin in normoglycaemic and NIDDM rat models and its implications on extra-pancreatic glucose regulation. *Diabetes Obes. Metab.*, **2008**, *10*(11), 1097-1104. <http://dx.doi.org/10.1111/j.1463-1326.2008.00869.x> PMID: 18355329
- Murugesan, N.; Woodard, K.; Ramaraju, R.; Greenway, F.L.; Coulter, A.A.; Rebello, C.J. Naringenin increases insulin sensitivity and metabolic rate: A case study. *J. Med. Food*, **2020**, *23*(3), 343-348. <http://dx.doi.org/10.1089/jmf.2019.0216> PMID: 31670603
- Fuor, E.V.; Mocanu, C.A.; Deleanu, M.; Voicu, C.; Anghelache, M.; Rebleanu, D.; Simionescu, M.; Calin, M. Evaluation of VCAM-1 targeted

- naringenin/indocyanine green-loaded lipid nanoemulsions as theranostic nanoplatfoms in inflammation. *Pharmaceutics*, **2020**, 12(11), 1066.
<http://dx.doi.org/10.3390/pharmaceutics12111066> PMID: 33182380
- [43] Rehman, K.; Khan, I.I.; Akash, M.S.H.; Jabeen, K.; Haider, K. Naringenin downregulates inflammation-mediated nitric oxide overproduction and potentiates endogenous antioxidant status during hyperglycemia. *J. Food Biochem.*, **2020**, e13422, e13422.
<http://dx.doi.org/10.1111/jfbc.13422> PMID: 32770581
- [44] Ye, G.; Wang, M.; Liu, D.; Cheng, L.; Yin, X.; Zhang, Q.; Liu, W. E. G.; Wang, M.; Liu, D.; Cheng, L.; Yin, X.; Zhang, Q.; Liu, W. Mechanism of naringenin blocking the protection of LTB4/BLT1 receptor against septic cardiac dysfunction. *Ann. Clin. Lab. Sci.*, **2020**, 50(6), 769-774.
 PMID: 33334792
- [45] Duda-Madej, A.; Kozłowska, J.; Krzyżek, P.; Aniol, M.; Seniuk, A.; Jermakow, K.; Dworniczek, E. Antimicrobial *O*-alkyl derivatives of naringenin and their oximes against multidrug-resistant bacteria. *Molecules*, **2020**, 25(16), 3642.
<http://dx.doi.org/10.3390/molecules25163642> PMID: 32785151
- [46] Clementi, N.; Scagnolari, C.; D'Amore, A.; Palombi, F.; Criscuolo, E.; Frasca, F.; Pierangeli, A.; Mancini, N.; Antonelli, G.; Clementi, M.; Carpaneto, A.; Filippini, A. Naringenin is a powerful inhibitor of SARS-CoV-2 infection *in vitro*. *Pharmacol. Res.*, **2021**, 163, 105255.
<http://dx.doi.org/10.1016/j.phrs.2020.105255> PMID: 33096221
- [47] Niu, X.; Sang, H.; Wang, J. Naringenin attenuates experimental autoimmune encephalomyelitis by protecting the intact of blood-brain barrier and controlling inflammatory cell migration. *J. Nutr. Biochem.*, **2021**, 89, 108560.
<http://dx.doi.org/10.1016/j.jnutbio.2020.108560> PMID: 33249188
- [48] Chen, W.; Lin, B.; Xie, S.; Yang, W.; Lin, J.; Li, Z.; Zhan, Y.; Gui, S.; Lin, B. Naringenin protects RPE cells from NaIO₃-induced oxidative damage *in vivo* and *in vitro* through up-regulation of SIRT1. *Phytomedicine*, **2021**, 80, 153375.
<http://dx.doi.org/10.1016/j.phymed.2020.153375> PMID: 33096452